IEEE Access
Multidisciplinary | Rapid Review | Open Access Journal

Received August 24, 2019, accepted September 16, 2019, date of publication September 19, 2019, date of current version October 1, 2019.

Digital Object Identifier 10.1109/ACCESS.2019.2942337

Joint Effects of Residual Hardware Impairments and Channel Estimation Errors on SWIPT Assisted Cooperative NOMA Networks

XINGWANG LI[1], (Member, IEEE), MENG LIU[1], (Student Member, IEEE), CHAO DENG[1], DI ZHANG[2,3], (Member, IEEE), XIANG-CHUAN GAO[2], KHALED M. RABIE[4], (Member, IEEE), AND RUPAK KHAREL[5], (Senior Member, IEEE)

[1]School of Physics and Electronic Information Engineering, Henan Polytechnic University, Jiaozuo 454000, China
[2]School of Information Engineering, Zhengzhou University, Zhengzhou 450001, China
[3]Information System Laboratory, Department of Electrical and Computer Engineering, Seoul National University, Seoul 08826, South Korea
[4]Faculty of Science and Engineering, Manchester Metropolitan University, Manchester M1 5GD, U.K.
[5]Department of Computing and Mathematics, Manchester Metropolitan University, Manchester M15 6BH, U.K.

Corresponding author: Chao Deng (super@hpu.edu.cn)

This work was supported in part by the Henan Scientific and Technological Research Project under Grant 182102210307, in part by the Doctoral Scientific Funds of Henan Polytechnic University under Grant B2016-34, in part by the Fundamental Research Funds for the Universities of Henan Province under Grant NSFRF180309, in part by the Outstanding Youth Science Foundation of Henan Polytechnic University under Grant J2019-4, in part by the Key Scientific Research Projects of Higher Education Institutions in Henan Province under Grant 20A510007, in part by the Research on Video Target Tracking Technology Based on Depth Learning Funds of Huaiyin Institute of Technology under Grant JSLERS-2018-005, and in part by the Research on Campus Security Application System Based on Artificial Intelligence Vision Technology under Grant NSFRF180411.

ABSTRACT In this paper, we investigate the effects of residual hardware impairments (RHIs), channels estimation errors (CEEs) and imperfect successive interference cancellation (ipSIC) on the cooperative non-orthogonal multiple access (NOMA) system over Nakagami-*m* channels, where the amplify-and-forward (AF) relay can harvest energy from the source. The exact expressions for outage probability and ergodic sum rate are derived in closed-form. In addition, the asymptotic outage analyses in the high signal-to-noise (SNR) regime are carried out. The results show that the outage probability exists an error floor due to the existence of CEEs and compared with RHIs, CEEs have a more serious impact on the system outage performance. The close simulation results of Monte Carlo verify the accuracy of our theoretical derivation. Finally, the performance of energy efficiency is examined with RHIs, CEEs and ipSIC.

INDEX TERMS NOMA, residual hardware impairments, SWIPT, imperfect successive interference cancellation.

I. INTRODUCTION

With the development of communication technology, the fifth generation (5G) mobile communication network has gradually entered the field of vision. Mobile Internet and Internet of things (IoTs) services will become the main driving forces of mobile communication development in the future 5G era [1]. Currently, communication networks primarily utilized orthogonal multiple access (OMA) technique [2]. The conventional OMA scheme needs to guarantee orthogonality of the resource to avoid interferences among users, such as time/frequency/code resources and has the disadvantage of low spectral efficiency and connectivity [3]. Although the orthogonal frequency division multiple access (OFDMA) technique can improve spectral efficiency by using overlapping subcarriers, it is still difficult to achieve the maximum Shannon capacity bound. In contract, power domain multiplexing, non-orthogonal multiple access (NOMA) can achieve higher spectral efficiency by serving multiple user in the same resource [4]. At transmitter, the signals are encoded by superposition coding and sent to destinations with different power levels. At the receiver, the signal can be separately detected by successive interference cancellation (SIC) [5], [6]. Moreover, NOMA can ensure the fairness of users by allocating more power to the users under weaker channel conditions and less power to the user under stronger channel conditions [7].

To enhance the reception reliability of far users, cooperative NOMA is proposed by introducing cooperative communication into NOMA [8]. In order to improve the performance of the cell-edge user, the authors proposed two cooperative NOMA relay schemes in [9], the results show that the proposed scheme can improve the outage performance of cell-edge users. To exploit the prior information of NOMA systems, the authors proposed a cooperative NOMA scheme in [10], the simulation results indicated that the

The associate editor coordinating the review of this manuscript and approving it for publication was Gurkan Tuna.

performance of cooperative NOMA systems is superior to the non-cooperative NOMA. Most of the above articles are based on the perfect SIC (pSIC), while the execution of pSIC requires extremely high precision receivers, which is obviously impossible in the real communication networks [11]. In [12], the authors studied the bit error rate performance of NOMA systems under the conditions of ideal and non-ideal SIC, and presented a more realistic method than the pSIC. The expressions of outage probability and throughput of code-domain NOMA (CD-NOMA)/power-domain NOMA (PD-NOMA) with pSIC/imperfect SIC (ipSIC) over Rayleigh fading channels in delay-limited transmission mode were derived in [13]. All of the works showed that the study of ipSIC is more relevant to the actual situation.

Simultaneous wireless information and power transfer (SWIPT) is an effective way to prolong the lifetime of energy-constrained wireless networks, such IoTs and vehicle-to-everything (V2X) [3], [14]. In the applications, the devices are deployed in remote areas or mobility, where the wireless devices are infeasible to support by power line [15]. In general, SWIPT are classified into two type of protocols, power splitting (PS) [16] and time switch (TS) [17]. In [18], authors studied the effects of SWIPT under both PS and TS schemes in MIMO wireless networks and presented the outer bound for the achievable rate-energy region. In [19], the system performances of both single-input single-output (SISO) and multiple-input single-output (MISO) SWIPT NOMA systems were studied and the results showed that the performance of SWIPT NOMA is better than that of NOMA, which indicated that SWIPT can provide higher gain for the system. Considering TS protocol, authors in [20] derived exact analytical expressions for the outage probability and network throughput of cooperative relaying systems.

Unfortunately, the main drawback of the above research works is that they assume all radio frequency (RF) components are perfect, which is over-realistic. In practice, by deploying low-cost and low power components, all RF front-ends are prone hardware imperfections, and they suffer from a variety of hardware impairments, such as phase noise, in phase/quadrature phase (I/Q) imbalance, high power amplifier nonlinearity and quantization error [21], [22]. To this end, a great deal of works have proposed many algorithms to compensate the loss caused by hardware impairments [23]–[25]. However, the residual hardware impairments have significant effects on the system performance, authors in [26] studied the system effects of multiple-relay AF network in the presence of RHIs and derived the closed-form expression of the outage probability. In [27], authors investigated the effects of RHIs on the NOMA system networks and proved that the outage performance of the system will be reduced sightly by RHIs at the low signal-to-noise ratios (SNRs).

In practical communication systems, due to the continuous movement of users, the path loss is uncertain, especially for the access of 5G massive users, it is a great challenge to obtain perfect channel state information (CSI) [28]. The common way to do this is to estimate channel at relay by the training sequence. In these cases, the channel estimation errors (CEEs) are thus inevitable due to the imperfection of estimation algorithms and some types of noise [29]. The effects of CEEs on multiple-input multiple-output (MIMO)-OFDM systems over Rayleigh fading channels were discussed in [30]. The influence of CEEs on the performance of wireless-powered with a DF relay over the Rayleigh channels was studied in [31]. The authors demonstrated that CEEs can reduce the performance of demodulator seriously and improve the bit error rate (BER) of the considered system [32]. Specifically, the authors in [33] considered a more practical system, where the joint effects of RHIs and CEEs on the AF cooperative system were investigated and it is proved that RHIs has a great negative influence on the system performance at high transmission rate, while CEEs has the opposite effect. The outage and the expected spectral efficiency performances of the cooperative DF systems in the presence of RHIs and CEEs were studied in [34]. Recently, in [35], the authors considered the performance of the NOMA system in the presence of both RHIs and CEEs, while the presence of direct link communication between the base station and the far users was not considered.

A. MOTIVATION AND CONTRIBUTIONS

The previous literature has provided solid foundation of cooperative NOMA, however the study on NOMA SWIPT AF systems in the presence of RHIs, ICSI and ipSIC is still invisible yet. In order to fill this gap, this paper makes an in-depth study of the joint effects of the three practical factors on the system performance. In particular, the Nakagami-m channel is adopted as our channel model. The reason is that Nakagami-m is a general fading channel, which can be used to capture some common fading channels. In this paper, the source node can transmit the supposed signals to the near users and the far users with the aid of an AF relay or through the direct connection. To intuitively reflect the state of communication, the exact analytical expressions of the outage probability and the approximate expressions at high SNRs are derived. In addition, the ergodic sum rate and energy efficiency in ideal and non-ideal conditions are calculated. The main contributions of this paper are summarized as follows:

- We consider a practical wireless communication system, where all transceivers suffer from hardware impairments and CSIs from all links are imperfect due to CEEs. Owing to the above ideal factors, the ipSIC at the receivers is taken into account.
- By considering the three deleterious factors, we investigate the outage performance of the considered system by deriving the closed-form analytical expressions of the outage probability for the far users and the near users.
- In order to obtain deeper insights, we derive the approximate outage probability in the high SNR region. The simulation results show that an error floor exists in

the non-ideal conditions. This happens because that the asymptotic outage performance is limited by the CEEs.

- We analyze the ergodic sum rate and energy efficiency of the considered system by deriving the closed-form expressions. The results indicate that, as the SNR increases, the ergodic sum rate and energy efficiency will increase all the time in the ideal conditions, while for the non-ideal conditions, due to the RHIs, ICSI and ipSIC, the ergodic rate and energy efficiency will reach the upper bound.

The remainder of this paper is organised as follows: Section II describes the system model by considering RHIs, ICSI and ipSIC. Section III presents the exact and asymptotic outage probability expressions of the far users and near users. In Section IV, the ergodic capacity of the far and near users are investigated. In Section V, we investigate the energy efficiency in both ideal and non-ideal conditions. Our analyses are proved by the numeric results in Section VI before the conclusion in Section VII.

B. NOTATION

Throughout this paper, $\Pr(\cdot)$ denotes probability for a random variable; $\triangleq$ represents definition operation; $\mathbb{E}(\cdot)$ symbolizes the expectation operator; the cumulative distribution function (CDF) and the probability density function (PDF) of a random variable X are represented by $F_X(\cdot)$ and $f_X(\cdot)$, respectively.

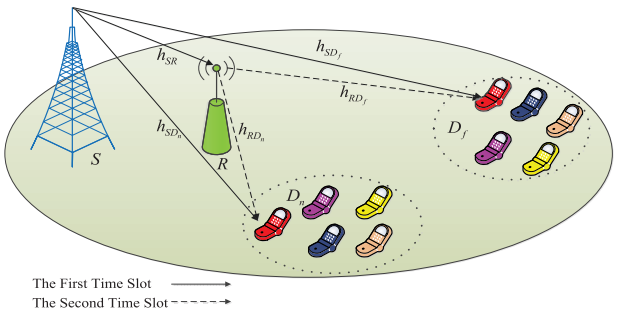

FIGURE 1. System model.

II. SYSTEM MODEL

As can be seen in FIGURE 1, we consider a NOMA SWIPT AF relaying network, which consists one source S, one relay R and M destinations $(D_1, D_2, \ldots D_M)$. Note that it is unrealistic to perform NOMA for all users. The practical way is to separate all users into multiple clusters, where users perform NOMA in the same cluster and OMA in the different clusters. To facilitate the analysis, users in the same cluster are divided into two groups, one is near user and another is far user.[1] In one cluster, S wants to send the signals s_1 and s_2 to the far users D_f and the near users D_n directly or with the aid of the AF relay where the signals satisfy with $\mathbb{E}\left[|s_1|^2\right] = \mathbb{E}\left[|s_2|^2\right] = 1$. Moreover, it is almost impossible to obtain the exact CSI. The practical way to obtain the channel knowledge is training by suing pilots. By using linear minimum mean square error (LMMSE) [36], the channel coefficient can be defined as $h_i = \hat{h}_i + e_i, i = \{SR, SD_f, SD_n, RD_f, RD_n\}$ where h_i and $\hat{h}_i$ denote the real channel coefficient and estimation channel coefficient, respectively. $e_i \sim \mathcal{CN}\left(0, \sigma_{e_i}^2\right)$ denotes the CEEs [37].[2] Without loss of generality, the estimated channel gains between the source and destinations are sorted as $\left|\hat{h}_{SD_1}\right|^2 \leq \left|\hat{h}_{SD_2}\right|^2 \leq \ldots \leq \left|\hat{h}_{SD_M}\right|^2$.

The whole process is divided into two phases: EH phase and signals transmission phase.

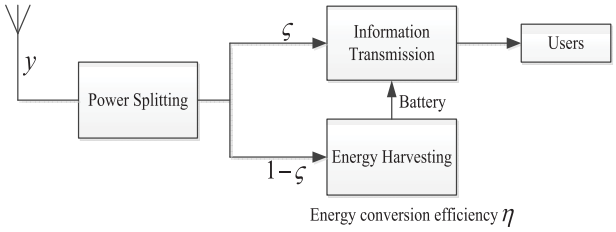

FIGURE 2. Power splitting protocol.

A. EH PHASE

In this paper, the power splitting protocol is adopted as shown in FIGURE 2, the transmit signal was split into two steams: one part of the power $(1-\varsigma)$ is used for EH and another part (ς) is used for information transmission, where ς is power allocation factor for information transmission. It is assumed that the total power transmitted from the source node is P_S, then the harvested energy at R can be expressed as

$$Q_{EH} = \eta(1-\varsigma)|h_{SR}|^2 P_S, \tag{1}$$

where $\eta \in [0, 1]$ denotes the energy conversion efficiency. In this phase, the RHIs and CEEs are not considered, as all non-ideal factors can be encompassed in η.

According to the PS protocol, the received power at the relay can be expressed as

$$P_R = \eta\varsigma|h_{SR}|^2 P_S. \tag{2}$$

B. SIGNALS TRANSMISSION PHASE

The signals transmission is divided into two time slots. In the first time slot, the superposed signals are simultaneously transmitted to destinations and relay. In the second time slot, the relay amplifies and forwards the signals to the destinations.

The first time slot: The source node S sends $\sqrt{a_1 P_S}s_1 + \sqrt{a_2 P_S}s_2$ to the relay R and the destinations D_f and D_n, where a_1 and a_2 represent the power coefficients of the transmission power for D_f and D_n with $a_1 + a_2 = 1$ and $a_1 > a_2$. Thus, the received signal at the relay and the users can be expressed as

$$y_{i_1} = \left(\hat{h}_{i_1} + e_{i_1}\right)\left(\sqrt{a_1 P_S}s_1 + \sqrt{a_2 P_S}s_2 + \eta_{t,i_1}\right) + \eta_{r,i_1} + v_{i_1}, \quad \left(i_1 = SR, SD_f, SD_n\right), \tag{3}$$

[1] In this paper, we only study signals of far user and near user in one cluster.

[2] Note that, the estimation channel and estimation are orthogonal [38] and the CEEs can be approximated as a Gaussian random variable [39].

where $v_{i_1} \sim \mathcal{CN}(0, N_0)$ denotes the additive white Gaussian noise (AWGN) at R; D_f and D_n, $\eta_{t,i_1} \sim \mathcal{CN}\left(0, \kappa_{t,i_1}^2 P_S\right)$ and $\eta_{r,i_1} \sim \mathcal{CN}\left(0, \kappa_{r,i_1}^2 P_S \left|h_{i_1}\right|^2\right)$ denote the distortion noises from the transmitter and receiver, respectively [40]. Combining the distribution of η_{t,i_1} and η_{r,i_1}, after some mathematical calculations, the received signal can be rewritten as

$$y_{i_1} = \left(\hat{h}_{i_1} + e_{i_1}\right)\left(\sqrt{a_1 P_S} s_1 + \sqrt{a_2 P_S} s_2 + \eta_{i_1}\right) + v_{i_1}, \quad (4)$$

where $\eta_{i_1} \sim \mathcal{CN}\left(0, \kappa_{i_1}^2 P_S\right)$ and $\kappa_{i_1} = \sqrt{\kappa_{t,i_1}^2 + \kappa_{r,i_1}^2}$.[3]

The second time slot: The relay amplifies and forwards the received signal to the destinations as

$$y_{i_2} = \left(G y_{SR} + \eta_{t,i_2}\right)\left(\hat{h}_{i_2} + e_{i_2}\right) + \eta_{r,i_2} + v_{i_2}, \quad \left(i_2 = RD_f, RD_n\right), \quad (5)$$

where $G = \sqrt{P_R / \left(\left(\rho_{SR}^2 + \sigma_{e_{SR}}^2\right)\left(1 + \kappa_{SR}^2\right) P_S + N_0\right)}$ represents the amplifying gain factor, $\eta_{t,i_2} \sim \mathcal{CN}\left(0, \kappa_{t,i_2}^2 P_R\right)$ and $\eta_{r,i_2} \sim \mathcal{CN}\left(0, \kappa_{r,i_2}^2 P_R \left|h_{i_2}\right|^2\right)$ denote the distortion noises, while $v_{i_2} \sim \mathcal{CN}(0, N_0)$ denotes AWGN. Similar to (4), we can rewrite (5) as

$$y_{i_2} = \left(\hat{h}_{i_2} + e_{i_2}\right)\left(G y_{SR} + \eta_{i_2}\right) + v_{i_2}. \quad (6)$$

where $\eta_{i_2} \sim \mathcal{CN}\left(0, \kappa_{i_2}^2 P_R\right)$ and $\kappa_{i_2} = \sqrt{\kappa_{t,i_2}^2 + \kappa_{r,i_2}^2}$.

C. FADING CHANNEL

In this study, we assume that the channel coefficient h_i follows Nakagami-m distribution. The PDF and CDF of the estimated channel gain $\rho_i = \left|\hat{h}_i\right|^2$ can be expressed as

$$f_{\rho_i}(x) = \frac{x^{\alpha_i - 1}}{\Gamma(\alpha_i)\beta_i^{\alpha_i}} e^{-\frac{x}{\beta_i}}, \quad (7)$$

$$F_{\rho_i}(x) = 1 - \sum_{g_i=0}^{\alpha_i - 1} \frac{e^{-\frac{x}{\beta_i}}}{g_i!}\left(\frac{x}{\beta_i}\right)^{g_i}, \quad (8)$$

where $\Gamma(\cdot)$ denotes the Gamma function, α_i and β_i are the multipath fading and the control spread parameters, respectively. Using the order statistics, the PDF and CDF of the m-th user estimated channel gain $\left|\hat{h}_m\right|^2$ can be expressed as [41]

$$f_{\rho_m}(x) = b_m f_{\rho_i}(x)\left[F_{\rho_i}(x)\right]^{m-1}\left[1 - F_{\rho_i}(x)\right]^{M-m}, \quad (9)$$

$$F_{\rho_m}(x) = b_m \sum_{z=0}^{M-m} \binom{M-m}{z} \frac{(-1)^z}{m+z}\left[F_{\rho_i}(x)\right]^{m+z}, \quad (10)$$

where $b_m = M!/\left((m-1)!\,(M-m)!\right)$.

[3] κ_{t,i_1} and κ_{r,i_1} represent the parameters of the magnitude of the mismatch between the desired signals and the actual received signals, for a given channel h, the power of the aggregated distortion at the receiver satisfies $\mathbb{E}_{\eta_{t/r}}\left[\left|h\eta_{t,i_1} + \eta_{r,i_1}\right|^2\right] = P_S|h|^2\left(\kappa_{t,i_1}^2 + \kappa_{r,i_1}^2\right)$.

During the first time slot, D_n first decodes the high intensity signal s_1 according to the NOMA protocol. Therefore, the received signal-to-interference-plus-noise ratio (SINR) for D_n to decode D_f's signal is given by

$$\gamma_{SD_n \to f} = \frac{a_1 \rho_{SD_n} \gamma}{\left(a_2 + \kappa_{SD_n}^2\right)\rho_{SD_n}\gamma + \left(\kappa_{SD_n}^2 + 1\right)\sigma_{e_{SD_n}}^2 \gamma + 1}, \quad (11)$$

where $\gamma = P_S/N_0$ denotes the transmit SNR at S. Owing to the ipSIC, the SINR of D_n to decode its own signal can be given as

$$\gamma_{SD_n} = \frac{a_2 \rho_{SD_n} \gamma}{\left(\kappa_{SD_n}^2 + a_1 \varepsilon\right)\rho_{SD_n}\gamma + \left(\kappa_{SD_n}^2 + 1\right)\sigma_{e_{SD_n}}^2 \gamma + 1}, \quad (12)$$

where the parameter ε ($0 \le \varepsilon \le 1$) denotes the level of residual interference due to that D_n cannot remove D_f's information.[4] In addition, it is worth noting that $\varepsilon = 0$ represents the system performs perfect SIC and $\varepsilon = 1$ represents that SIC is not implemented in the system. The received SINR of the user D_f is given by

$$\gamma_{SD_f} = \frac{a_1 \rho_{SD_f} \gamma}{\left(a_2 + \kappa_{SD_f}^2\right)\rho_{SD_f}\gamma + \left(\kappa_{SD_f}^2 + 1\right)\sigma_{e_{SD_f}}^2 \gamma + 1}. \quad (13)$$

During the second time slot, the received SINR of user D_f is given by

$$\gamma_{RD_f} = \frac{\rho_{SR}\rho_{RD_f} a_1 \gamma \gamma'}{\rho_{SR}\rho_{RD_f}\left(a_2 + d_1\right)\gamma\gamma' + \rho_{RD_f}\gamma'\varphi_2 + \rho_{SR}\gamma\varphi_1 + \varphi_3}, \quad (14)$$

where $\gamma' = P_R/N_0$ denotes the transmit SNR at R, $d_1 = \kappa_{SR}^2 + \kappa_{RD_f}^2 + \kappa_{SR}^2\kappa_{RD_f}^2$, $\varphi_1 = \sigma_{e_{RD_f}}^2\left(d_1 + 1\right)\gamma' + \kappa_{SR}^2 + 1$, $\varphi_2 = \sigma_{e_{SR}}^2\left(d_1 + 1\right)\gamma + \kappa_{RD_f}^2 + 1$, $\varphi_3 = \sigma_{e_{SR}}^2\sigma_{e_{RD_f}}^2\left(d_1 + 1\right)\gamma\gamma' + \sigma_{e_{RD_f}}^2\left(\kappa_{RD_f}^2 + 1\right)\gamma' + \sigma_{e_{SR}}^2\left(\kappa_{RD_f}^2 + 1\right)\gamma + 1$.

By considering ipSIC, the SINRs for D_n to decode D_f's signal and its own signal are respectively expressed as

$$\gamma_{RD_n \to f} = \frac{\rho_{SR}\rho_{RD_n} a_1 \gamma \gamma'}{\rho_{SR}\rho_{RD_n}\left(a_2 + d_2\right)\gamma\gamma' + \rho_{RD_n}\gamma'\varphi_4 + \rho_{SR}\gamma\varphi_5 + \varphi_6}, \quad (15)$$

$$\gamma_{RD_n} = \frac{\rho_{SR}\rho_{RD_n} a_2 \gamma \gamma'}{\rho_{SR}\rho_{RD_n}\left(d_2 + \varepsilon a_1\right)\gamma\gamma' + \rho_{RD_n}\gamma'\varphi_4 + \rho_{SR}\gamma\varphi_5 + \varphi_6}, \quad (16)$$

where $d_2 = \kappa_{SR}^2 + \kappa_{RD_n}^2 + \kappa_{SR}^2\kappa_{RD_n}^2$, $\varphi_4 = \sigma_{e_{SR}}^2\left(d_2 + 1\right)\gamma + \kappa_{RD_n}^2 + 1$, $\varphi_5 = \sigma_{e_{RD_n}}^2\left(d_2 + 1\right)\gamma' + \kappa_{SR}^2 + 1$, $\varphi_6 = \sigma_{e_{SR}}^2\sigma_{e_{RD_n}}^2\left(d_2 + 1\right)\gamma\gamma' + \sigma_{e_{SR}}^2\left(\kappa_{SR}^2 + 1\right)\gamma + \sigma_{e_{RD_n}}^2\left(\kappa_{RD_n}^2 + 1\right)\gamma' + 1$. When $\kappa_{SR} = \kappa_{RD_f} = \kappa_{RD_n} = \kappa_{SD_n} = \kappa_{SD_f} = 0$, $\sigma_{e_{SR}} = \sigma_{e_{RD_f}} = \sigma_{e_{RD_n}} = \sigma_{e_{SD_n}} = \sigma_{e_{SD_f}} = 0$ and $\varepsilon = 0$ are established, (11)-(16) simplified to ideal conditions.

[4] The parameter of ipSIC ε follows Gaussian distribution [42] and we assume that ε is a fixed value for simplicity in this paper.

III. OUTAGE PROBABILITY ANALYSIS

In this section, the outage probability of D_f and D_n are derived to analyze the performance of the considered system. In order to obtain more insights, we also analyze the asymptotic behavior of outage probability in the high SNR region.

A. EXACT OUTAGE PROBABILITY

An outage event will occur at D_f if the SINRs of the signal transmitted by the source node and the relay node cannot reach the target threshold γ_{thf}. Thus, the outage probability for D_f can be expressed as

$$\mathrm{P}_{out}^{D_f} = \underbrace{\Pr(\gamma_{SD_f} < \gamma_{thf})}_{I_1} \underbrace{\Pr(\gamma_{RD_f} < \gamma_{thf})}_{I_2}. \tag{17}$$

The exact expression of D_f's outage probability is given in the following theorem.

Theorem 1: The closed-form expression for the outage probability of the far user is expressed as

$$\begin{aligned} P_{out}^{D_f} &= b_f \sum_{z=0}^{M-f} \binom{M-f}{z} \frac{(-1)^z}{f+z} \left[1 - \sum_{g_5=0}^{\alpha_{SD_f}-1} \frac{e^{-\frac{\theta_2}{\beta_{SD_f}}}}{g_5!} \left(\frac{\theta_2}{\beta_{SD_f}} \right)^{g_5} \right]^{f+z} \\ &\times \left[1 - \frac{2}{\Gamma(\alpha_{SR}) \beta_{SR}^{\alpha_{SR}}} e^{-\frac{\theta_1}{\beta_{SR}} - \frac{\gamma\varphi_1\theta_1}{\beta_{RD_f}\gamma_2\varphi_2}} \sum_{g_2=0}^{\alpha_{RD_f}-1} \frac{1}{g_2!} \sum_{u=0}^{\alpha_{SR}-1} \binom{\alpha_{SR}-1}{u} \right. \\ &\times \sum_{q=0}^{g_2} \binom{g_2}{q} \theta_1^{\alpha_{SR}+g_2-\frac{u+q+1}{2}} \left(\frac{1}{\beta_{RD_f}\gamma'\varphi_2} \right)^{g_2+\frac{u-q+1}{2}} (\theta_1\gamma\varphi_1+\varphi_3)^{\frac{u+q+1}{2}} \\ &\left. \times (\gamma\varphi_1)^{g_2-q} \beta_{SR}^{\frac{u-q+1}{2}} K_{u-q+1} \left(2\sqrt{\frac{\theta_1(\theta_1\gamma\varphi_1+\varphi_3)}{\beta_{SR}\beta_{RD_f}\gamma'\varphi_2}} \right) \right], \end{aligned} \tag{18}$$

where $b_f = M!/((f-1)!(M-f)!)$ and f denotes the f-th user (far user), $\theta_1 = \varphi_2\gamma_{thf} / \left(a_1\gamma - (a_2+d_1)\gamma\gamma_{thf}\right)$, $\theta_2 = \left(\left(\kappa_{SD_f}^2+1\right)\sigma_{e_{SD_f}}^2\gamma\gamma_{thf} + \gamma_{thf}\right) / \left(a_1\gamma - \left(a_2+\kappa_{SD_f}^2\right)\gamma\gamma_{thf}\right)$ with $a_1 > (a_2+d_1)\gamma_{thf}$ and $a_1 > \left(a_2+\kappa_{SD_f}^2\right)\gamma_{thf}$, $K_v(\cdot)$ denotes the modified Bessel function of the second kind with order v.

Proof: See Appendix A. □

The outage event will occur at D_n for two scenarios: *i)* D_n cannot decode D_f's signal successfully; and *ii)* D_n fails to decode its own signal. Hence, the outage probability of D_n can be expressed as

$$\begin{aligned} \mathrm{P}_{out}^{D_n} = &\underbrace{\left[1 - \Pr\left(\gamma_{RD_{n\to f}} > \gamma_{thf}, \gamma_{RD_n} > \gamma_{thn}\right)\right]}_{I_3} \\ &\times \underbrace{\left[1 - \Pr\left(\gamma_{SD_{n\to f}} > \gamma_{thf}, \gamma_{SD_n} > \gamma_{thn}\right)\right]}_{I_4}, \end{aligned} \tag{19}$$

where γ_{thn} denotes the target threshold at D_n.

The exact expression of D_n's outage probability is given in the following theorem.

Theorem 2: The closed-form expression for the outage probability of the near user is expressed as

$$\begin{aligned} P_{out}^{D_n} &= b_n \sum_{z=0}^{M-n} \binom{M-n}{z} \frac{(-1)^z}{n+z} \left[1 - \sum_{g_4=0}^{\alpha_{SD_n}-1} \frac{e^{-\frac{\tau}{\beta_4}}}{g_4!} \left(\frac{\tau}{\beta_{SD_n}} \right)^{g_4} \right]^{n+z} \\ &\times \left[1 - \frac{2}{\Gamma(\alpha_{SR}) \beta_{SR}^{\alpha_{SR}}} \sum_{g_3=0}^{\alpha_{RD_n}-1} \frac{1}{g_3!} \sum_{v=0}^{\alpha_{SR}-1} \binom{\alpha_{SR}-1}{v} e^{-\frac{\lambda}{\beta_{SR}} - \frac{\lambda\gamma\varphi_5}{\beta_{RD_n}\gamma'\varphi_4}} \right. \\ &\times \sum_{t=0}^{g_3} \binom{g_3}{t} (\gamma\varphi_5)^{g_3-t} (\lambda\gamma\varphi_5+\varphi_6)^{\frac{v+t+1}{2}} \beta_{SR}^{\frac{v-t+1}{2}} \lambda^{g_3+\alpha_{SR}-\frac{v+t+1}{2}} \\ &\left. \times \left(\frac{1}{\beta_{RD_n}\gamma'\varphi_4} \right)^{g_3+\frac{v-t+1}{2}} K_{v-t+1} \left(2\sqrt{\frac{\lambda(\lambda\gamma\varphi_5+\varphi_6)}{\beta_{SR}\beta_{RD_n}\gamma'\varphi_4}} \right) \right], \end{aligned} \tag{20}$$

where $b_n = M!/((n-1)!(M-n)!)$ and n denotes the n-th user (near user). $\tau \triangleq \max(\tau_1, \tau_2)$ and $\tau_1 = \left(\left(\kappa_{SD_n}^2+1\right)\sigma_{e_{SD_n}}^2\gamma\gamma_{thf} + \gamma_{thf}\right) / \left(a_1\gamma - \left(a_2+\kappa_{SD_n}^2\right)\gamma\gamma_{thf}\right)$, $\tau_2 = \left(\left(\kappa_{SD_n}^2+1\right)\sigma_{e_{SD_n}}^2\gamma\gamma_{thn} + \gamma_{thn}\right) / \left(a_2\gamma - \left(a_1\varepsilon + \kappa_{SD_n}^2\right)\gamma\gamma_{thn}\right)$; $\lambda \triangleq \max(\lambda_1, \lambda_2)$ and $\lambda_1 = \varphi_4\gamma_{thf} / \left(a_1\gamma - \left(a_2+d_2\right)\gamma\gamma_{thf}\right)$, $\lambda_2 = \varphi_4\gamma_{thn} / \left(a_2\gamma - (a_1\varepsilon + d_2)\gamma\gamma_{thn}\right)$. Note that all the conditions that make the equation establish are $a_1 > \left(a_2+\kappa_{SD_n}^2\right)\gamma_{thf}$, $a_2 > \left(\kappa_{SD_n}^2 + a_1\varepsilon\right)\gamma_{thn}$, $a_1 > (a_2+d_2)\gamma_{thf}$ and $a_2 > (a_1+d_2)\varepsilon\gamma_{thn}$.

Proof: See Appendix B. □

B. ASYMPTOTIC OUTAGE BEHAVIOR

In order to obtain more insights, the asymptotic outage performances for D_f and D_n are investigated in this subsection. At high SNRs, the asymptotic PDF and CDF of the channel gain $\rho_i = \left|\hat{h}_i\right|^2$ are given as [43]

$$f_{\rho_i}^{\infty}(x) \approx \frac{x^{\alpha_i}}{\alpha_i! \beta_i^{\alpha_i}}, \tag{21}$$

$$F_{\rho_i}^{\infty}(x) = \frac{M!}{m!(M-m)!} \left(\frac{1}{\alpha_i!} \right)^m \left(\frac{x}{\beta_i} \right)^{\alpha_i m}. \tag{22}$$

In the following corollaries, we describe the asymptotic expressions of outage probability of both near users and far users in ideal and non-ideal conditions.

Corollary 1: At high SNRs, the asymptotic expressions of outage probability for D_f are expressed as

- *Ideal conditions* ($\kappa = \sigma_e = \varepsilon = 0$)

$$\begin{aligned} P_{D_f}^{\infty,id} \approx b_f^{\infty} &\left(\frac{1}{\alpha_{SD_f}!} \right)^f \left(\frac{\theta_2}{\beta_{SD_f}} \right)^{\alpha_{SD_f} f} \left[\frac{1}{\alpha_{SR}! \beta_{SR}^{\alpha_{SR}}} \left(\frac{\varphi_2 b_1}{\gamma} \right)^{\alpha_{SR}} \right. \\ &\left. + \frac{1}{\alpha_{RD_f}! \beta_{RD_f}^{\alpha_{RD_f}}} \left(\frac{\varphi_1 b_1}{\gamma'} \right)^{\alpha_{RD_f}} \right]. \end{aligned} \tag{23}$$

- *Non-ideal conditions* ($\kappa, \sigma_e, \varepsilon \neq 0$)

$$P_{D_f}^{\infty,ni} \approx b_f^{\infty} \sum_{z=0}^{M-f} \binom{M-f}{z} \frac{(-1)^z}{f+z} \left[1 - \sum_{g_5=0}^{\alpha_{SD_f}-1} \frac{e^{-\frac{\theta_2'}{\beta_{SD_f}}}}{g_5!} \times \left(\frac{\theta_2'}{\beta_{SD_f}} \right)^{g_5} \right]^{f+z} \left[1 - \frac{2}{\Gamma(\alpha_{SR}) \beta_{SR}^{\alpha_{SR}}} e^{-\frac{\theta_1'}{\beta_{SR}} - \frac{\sigma_{e_{RD_f}}^2 \theta_1'}{\beta_{RD_f} \sigma_{e_{SR}}^2}} \times \sum_{g_2=0}^{\alpha_{RD_f}-1} \frac{1}{g_2!} \sum_{j=0}^{\alpha_{SR}-1} \binom{\alpha_{SR}-1}{j} \sum_{t=0}^{g_2} \binom{g_2}{t} \beta_{SR}^{\frac{j-t+1}{2}} \times {\theta_1'}^{\alpha_{SR}+g_2-\frac{j+t+1}{2}} \left(\frac{\sigma_{e_{RD_f}}^2}{\beta_{RD_f} \sigma_{e_{SR}}^2} \right)^{g_2+\frac{j-t+1}{2}} \left(\theta_1' + \sigma_{e_{SR}}^2 \right)^{\frac{j+t+1}{2}} \times K_{j-q+1} \left(2 \sqrt{\frac{\theta_1' \sigma_{e_{RD_f}}^2 \left(\theta_1' + \sigma_{e_{SR}}^2 \right)}{\beta_{SR} \beta_{RD_f} \sigma_{e_{SR}}^2}} \right) \right], \quad (24)$$

where $b_f^{\infty} = M!/\left((M-f)!M!\right)$, $b_1 = \gamma_{thf}/\left(a_1 - \left(a_2 + d_1\right)\gamma_{thf}\right)$, $\theta_1' = \sigma_{e_{RD_f}}^2 \left(d_1+1\right)\gamma_{thf}/\left(a_1 - \left(a_2+d_1\right)\gamma_{thf}\right)$, $\theta_2' = \left(\kappa_{SD_f}^2 + 1\right)\sigma_{e_{SD_f}}^2 \gamma_{thf}/\left(a_1 - \left(a_2 + \kappa_{SD_f}^2\right)\gamma_{thf}\right)$.

Proof: See Appendix C. □

Corollary 2: At high SNRs, the asymptotic expressions of outage probability for D_n are expressed as

- *Ideal conditions* ($\kappa = \sigma_e = \varepsilon = 0$)

$$P_{D_n}^{\infty,id} \approx b_n^{\infty} \left(\frac{1}{\alpha_{SD_n}!} \right)^n \left(\frac{\tau}{\beta_{SD_n}} \right)^{\alpha_{SD_n} n} \left(\frac{\psi^{\alpha_{SR}}}{\alpha_{SR}! \beta_{SR}^{\alpha_{SR}}} + \frac{\xi^{\alpha_{RD_n}}}{\alpha_{RD_n}! \beta_{RD_n}^{\alpha_{RD_n}}} \right). \quad (25)$$

- *Non-ideal conditions* ($\kappa, \sigma_e, \varepsilon \neq 0$)

$$P_{D_n}^{\infty,ni} \approx b_n^{\infty} \sum_{z=0}^{M-n} \binom{M-n}{z} \frac{(-1)^z}{n+z} \left[1 - \sum_{g_4=0}^{\alpha_{SD_n}-1} \frac{e^{-\frac{\tau'}{\beta_{SD_n}}}}{g_4!} \times \left(\frac{\tau'}{\beta_{SD_n}} \right)^{g_4} \right]^{n+z} \left[1 - \frac{2}{\Gamma(\alpha_{SR}) \beta_{SR}^{\alpha_{SR}}} e^{-\frac{\lambda'}{\beta_{SR}} - \frac{\lambda' \sigma_{e_{RD_n}}^2}{\beta_{RD_n} \sigma_{e_{SR}}^2}} \times \sum_{g_3=0}^{\alpha_{RD_n}-1} \frac{1}{g_3!} \sum_{u=0}^{\alpha_{SR}-1} \binom{\alpha_{SR}-1}{u} \sum_{v=0}^{g_3} \binom{g_3}{v} \beta_{SR}^{\frac{u-v+1}{2}} \times {\lambda'}^{g_3+\alpha_{SR}-\frac{u+v+1}{2}} \left(\frac{\sigma_{e_{RD_n}}^2}{\beta_{RD_n} \sigma_{e_{SR}}^2} \right)^{g_3+\frac{u-v+1}{2}} \left(\lambda' + \sigma_{e_{SR}}^2 \right)^{\frac{u+v+1}{2}} \times K_{u-v+1} \left(2 \sqrt{\frac{\lambda' \sigma_{e_{RD_n}}^2 \left(\lambda' + \sigma_{e_{SR}}^2 \right)}{\beta_{SR} \beta_{RD_n} \sigma_{e_{SR}}^2}} \right) \right], \quad (26)$$

where $b_n^{\infty} = M!/\left((M-n)!M!\right)$, $\psi = \max\left(\psi_1, \psi_2\right)$, $\psi_1 = \varphi_4 b_2/\gamma$, $\psi_2 = \varphi_4 b_3/\gamma$; $\xi = \max\left(\xi_1, \xi_2\right)$, $\xi_1 = \varphi_5 b_2/\gamma'$, $\xi_2 = \varphi_5 b_3/\gamma'$ and $b_2 = \gamma_{thf}/\left(a_1 - \left(a_2+d_2\right)\gamma_{thf}\right)$, $b_3 = \gamma_{thn}/\left(a_2 - \left(a_1\varepsilon + d_2\right)\gamma_{thn}\right)$; $\tau' = \max\left(\tau_1', \tau_2'\right)$, $\tau_1' = \left(\kappa_{SD_n}^2 + 1\right)\sigma_{e_{SD_n}}^2 \gamma_{thf}/\left(a_1 - \left(a_2 + \kappa_{SD_n}^2\right)\gamma_{thf}\right)$, $\tau_2' = \left(\kappa_{SD_n}^2 + 1\right)\sigma_{e_{SD_n}}^2 \gamma_{thn}/\left(a_2 - \left(\kappa_{SD_n}^2 + a_1\varepsilon\right)\gamma_{thn}\right)$; $\lambda' = \max\left(\lambda_1', \lambda_2'\right)$, $\lambda_1' = b_2 \sigma_{e_{SR}}^2 \left(d_2+1\right)$, $\lambda_2' = b_3 \sigma_{e_{SR}}^2 \left(d_2+1\right)$.

Proof: See Appendix D. □

Remark 1: Corollary 1 and Corollary 2 provide some insights on the derived analytical results. The results show the effects of channel fading parameters and non-ideal factors on asymptotic outage performance intuitively. For the ideal conditions, the parameters of RHIs, CEEs and ipSIC are all reduced to 0, and the asymptotic outage probability decreases with the increase of SNR, especially in the high SNR regime, the outage probability increases almost linearly. While for non-ideal conditions, RHIs, CEEs and ipSIC have detrimental effects on the outage performance of the considered system. Moreover, the outage probability tends to be a fixed constant value with the increase of SNR which is due to the existence of CEEs. We can conclude that for the non-ideal conditions, the outage probability of the considered system depends on the channel fading parameters, distortion noise, CEEs and the performance of SIC, while the outage probability only depends on the channel fading parameters in the ideal conditions.

IV. ERGODIC SUM RATE

The ergodic capacity is the time average of the maximum information rate of the random channel in all fading states which can well reflect the fading performance of the system. Thus, in this section, we study the ergodic sum rate of the considered system.

The achievable rate of D_f and D_n can be expressed as

$$R_f = \frac{1}{2} \log_2 \left(1 + \max\left[\gamma_{SD_f}, \gamma_{RD_f}\right]\right), \quad (27)$$

$$R_n = \begin{cases} \frac{1}{2} \log_2 \left(1 + \max\left[\gamma_{SD_n}, \gamma_{RD_n}\right]\right), \text{if} \rho_{RD_n} > \rho_{RD_f} \\ \frac{1}{2} \log_2 \left(1 + \gamma_{SD_n}\right), \text{if } \rho_{RD_n} < \rho_{RD_f}. \end{cases} \quad (28)$$

where 1/2 indicates that the communication process is divided into two time slots. It is difficult to derive the exact expression of the ergodic sum rate, thus, in this paper, we only study the approximate expression of the ergodic sum rate in high SNR regime.

The ergodic rate of the D_f can be expressed as

- *Ideal conditions* ($\kappa = \sigma_e = \varepsilon = 0$)

$$R_{ave}^{f,id} = \mathbb{E}\left[\frac{1}{2} \log_2 \left(1 + \max\left[\gamma_{SD_f}, \gamma_{RD_f}\right]\right) \right], \quad (29)$$

when $\gamma, \gamma' \to \infty$, substituting (13) and (14) into(29), after some mathematical calculations the ergodic rate of D_f can be rewritten as

$$R_{ave}^{f,id} \approx \frac{1}{2} \log_2 \left(1 + \frac{a_1}{a_2}\right). \quad (30)$$

- *Non-ideal conditions* ($\kappa, \sigma_e, \varepsilon \neq 0$)

$$R_{ave}^{f,nid} \approx \frac{1}{2}\log_2\left(1+\max\left[\frac{a_1\Lambda_1}{a_2\Lambda_5+\kappa_{SD_f}^2\Lambda_5+\chi_5}, \frac{a_1\Lambda_1\Lambda_5}{(a_2+d_2)\Lambda_1\Lambda_2+\chi_6\Lambda_2+\chi_7\Lambda_1+\chi_8}\right]\right), \quad (31)$$

where $\chi_5 = \left(\kappa_{SD_f}^2+1\right)\sigma_{e_{SD_f}}^2$, $\chi_6 = \sigma_{e_{SR}}^2(d_1+1)$, $\chi_7 = \sigma_{e_{RD_f}}^2(d_1+1)$, $\chi_8 = \sigma_{e_{SR}}^2\sigma_{e_{RD_f}}^2(d_1+1)$, $\Lambda_1 = (\alpha_{SR}+1)\beta_{SR}$, $\Lambda_5 = \left(\alpha_{SD_f}+1\right)\beta_{SD_f}$, Λ_2 can be expressed as

$$\Lambda_2 = \frac{b_f\Gamma(c_2)}{\Gamma\left(\alpha_{RD_f}\right)\beta_{RD_f}^{\alpha_{RD_f}}}\sum_{t=0}^{f-1}\binom{f-1}{t}(-1)^t \sum_{p_0+\cdots+p_{\alpha_{RD_f}-1}=c_1} \times\binom{c_1}{p_0,\cdots,p_{\alpha_{RD_f}-1}}\prod_{g_2=0}^{\alpha_{RD_f}-1}\left(\frac{1}{g_2!}\right)^{p_{g_2}}\left(\frac{1}{\beta_{RD_f}}\right)^{g_2p_{g_2}}\left(\frac{c_1+1}{\beta_{RD_f}}\right)^{-c_2}, \quad (32)$$

where $c_1 = M-f+t$, $c_2 = g_2p_{g_2}+\alpha_{RD_f}-1$.

Proof: See Appendix E. □

The ergodic rate of the near users can be expressed as

- *Ideal conditions* ($\kappa = \sigma_e = \varepsilon = 0$)

$$R_{ave}^{n,id} = \Pr\left(\rho_{RD_n} > \rho_{RD_f}\right)\underbrace{\mathbb{E}\left[\frac{1}{2}\log_2\left(1+\max\left[\gamma_{SD_n},\gamma_{RD_n}\right]\right)\right]}_{R_{ave}^{n_1,id}} + \Pr\left(\rho_{RD_n} < \rho_{RD_f}\right)\underbrace{\mathbb{E}\left[\frac{1}{2}\log_2\left(1+\gamma_{SD_n}\right)\right]}_{R_{ave}^{n_2,id}}. \quad (33)$$

As for D_n, ρ_{RD_n} and ρ_{RD_f} are independent random variables, we thus assume $\Pr\left(\rho_{RD_n} > \rho_{RD_f}\right) = \Pr\left(\rho_{RD_n} < \rho_{RD_f}\right) = 1/2$. The ergodic rate of D_n can be rewritten as

$$R_{ave}^{n,id} = \frac{a_2b_n}{4\ln 2}\sum_{z=0}^{M-n}\binom{M-n}{z}\frac{(-1)^z}{n+z}\left[a_2\left(\Phi_1+\Phi_2-\Phi_3\right)-\Phi_4\right]. \quad (34)$$

- *Non-ideal conditions* ($\kappa, \sigma_e, \varepsilon \neq 0$)

$$R_{ave}^{n,nid} \approx \frac{1}{4}\log_2\left(1+\frac{a_2\Lambda_4}{\left(\kappa_{SD_n}^2+a_1\varepsilon\right)\Lambda_4+\chi_1}\right) + \frac{1}{4}\log_2\left(1+\max\left[\frac{a_2\Lambda_4}{\left(\kappa_{SD_n}^2+a_1\varepsilon\right)\Lambda_4+\chi_1}, \frac{a_1\Lambda_1\Lambda_2}{(a_1\varepsilon+d_2)\Lambda_1\Lambda_3+\chi_2\Lambda_3+\chi_3\Lambda_1+\chi_4}\right]\right), \quad (35)$$

where $\chi_1 = \left(\kappa_{SD_n}^2+1\right)\sigma_{e_{SD_n}}^2$, $\chi_2 = \sigma_{e_{SR}}^2(d_2+1)$, $\chi_3 = \sigma_{e_{RD_n}}^2(d_2+1)$, $\chi_4 = \sigma_{e_{SR}}^2\sigma_{e_{RD_f}}^2(d_2+1)$, $\Lambda_4 = \left(\alpha_{SD_n}+1\right)\beta_{SD_n}$, Λ_3 can be expressed as

$$\Lambda_3 = \frac{b_n\Gamma(c_4)}{\Gamma\left(\alpha_{RD_n}\right)\beta_{RD_n}^{\alpha_{RD_n}}}\sum_{q=0}^{n-1}\binom{n-1}{q}(-1)^q \sum_{p_0+\cdots+p_{\alpha_{RD_n}-1}=c_3} \times\binom{c_3}{p_0,\cdots,p_{\alpha_{RD_n}-1}}\prod_{g_3=0}^{\alpha_{RD_n}-1}\left(\frac{1}{g_3!}\right)^{p_{g_3}}\left(\frac{1}{\beta_{RD_n}}\right)^{g_3p_{g_3}}\left(\frac{c_3+1}{\beta_{RD_n}}\right)^{-c_4}, \quad (36)$$

where $c_3 = M-n+q$, $c_4 = g_3p_{g_3}+\alpha_{RD_n}-1$.

Proof: See Appendix F. □

According to the above results, we can get the ergodic sum rate in two conditions as follows:

- *Ideal conditions* ($\kappa = \sigma_e = \varepsilon = 0$)

$$R_{ave}^{sum\_id} \approx \frac{1}{2}\log_2\left(1+\frac{a_1}{a_2}\right)+\frac{a_2b_n}{4\ln 2}\sum_{z=0}^{M-n}\binom{M-n}{z} \times\frac{(-1)^z}{n+z}\left[a_2\left(\Phi_1+\Phi_2-\Phi_3\right)-\Phi_4\right]. \quad (37)$$

- *Non-ideal conditions* ($\kappa, \sigma_e, \varepsilon \neq 0$)

The ergodic sum rate for the users is given at the bottom of this page.

V. ENERGY EFFICIENCY

Energy efficiency is another important metric to evaluate the performance of wireless communication system. It refers

$$R_{ave}^{sum\_nid} = \frac{1}{4}\log_2\left(1+\frac{a_2\Lambda_4}{\kappa_{SD_n}^2\Lambda_4+\chi_5+a_1\varepsilon\Lambda_4}\right) + \frac{1}{4}\log_2\left(1+\max\left[\frac{a_2\Lambda_4}{\kappa_{SD_n}^2\Lambda_4+\chi_5+a_1\varepsilon\Lambda_4}, \frac{a_2\Lambda_1\Lambda_3}{d_2\Lambda_1\Lambda_3+\chi_6\Lambda_3+\chi_7\Lambda_1+\chi_8+a_1\varepsilon\Lambda_1\Lambda_3}\right]\right) + \frac{1}{2}\log_2\left(1+\max\left[\frac{a_1\Lambda_5}{a_2\Lambda_5+\kappa_{SD_f}^2\Lambda_5+\chi_1}, \frac{a_1\Lambda_1\Lambda_2}{a_2\Lambda_1\Lambda_2+d_1\Lambda_1\Lambda_2+\chi_2\Lambda_2+\chi_3\Lambda_1+\chi_4}\right]\right) \quad (38)$$

to the useful information transmitted to the receivers by each unit of energy consumed by the transmitters, which is expressed as [44]

$$\eta_{ee} = \frac{R_i}{Q_{total}}, \tag{39}$$

where R_i denotes the achievable rate of the i-th user, and Q_{total} denotes the total energy consumption. Q_{total} can be expressed as

$$Q_{total} = P_S + P_R + P_C, \tag{40}$$

where P_C is the fixed energy consumption which caused by transmitter and the receiver.

VI. NUMERICAL RESULTS

In this section, the correctness of our theoretical analysis is verified by the Monte-Carlo simulation. For the purpose of comparison, the performance of the system in the ideal conditions is also provided. The main parameters for the simulation are provided in Table 1.

TABLE 1. Simulation parameters.

Parameter	Value	Parameter	Value	Parameter	Value
α_i	2	β_i	0.1	M	2
m	2	f	1	η	0.4
γ_{thf}	1	γ_{thn}	3	ς	0.9
a_1	0.6	a_2	0.4	N_0	1
P_S	$10W$	P_C	$0.1W$		
σ_{e_i} (id)	0	κ_i (id)	0	ε (id)	0
σ_{e_i} (nid)	0.05	κ_i (nid)	0.1	ε (nid)	0.01

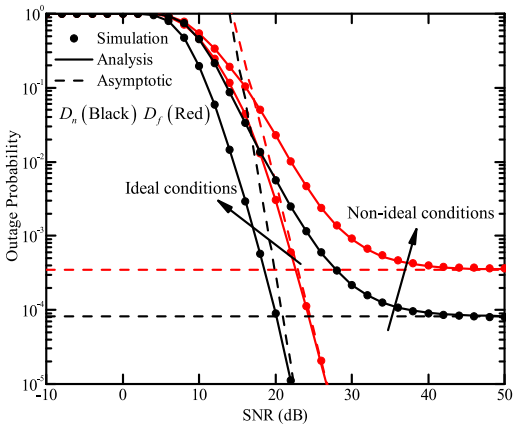

FIGURE 3. Outage probability of users versus transmit SNR in different conditions.

FIGURE 3 plots the outage probability versus the transmit SNR for ideal conditions $(\kappa_i = \sigma_{e_i} = \varepsilon = 0)$ and non-ideal conditions $(\kappa, \sigma_e, \varepsilon \neq 0)$. From FIGURE 3, we can see that the simulated results are completely coincident with the theoretical analysis values, which proves the correctness of our theoretical analysis. In the ideal conditions, we can see that the outage probability is always reducing without limited, while the outage probability gradually becomes stable in the non-ideal conditions. The reason is that in the ideal conditions, as the SNR increases, there are more desirable transmission signals, while in the non-ideal conditions, the outage probability is nearly a fixed value due to the CEEs (we will explain the reason in the next diagram). The results show that system performance cannot be always improved by increasing the SNR in non-ideal conditions.

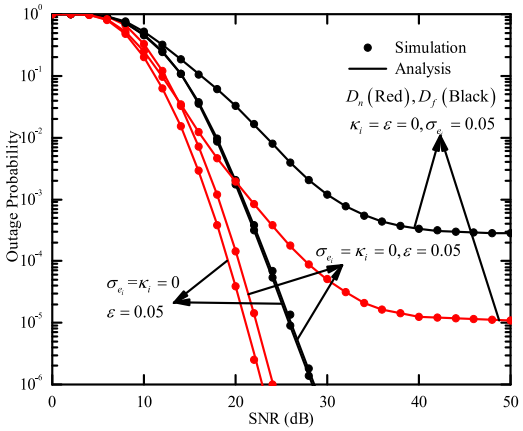

FIGURE 4. Outage probability of users versus different non-ideal factors.

FIGURE 4 presents the effect of non-ideal factors on the outage probability in three different situations $\sigma_{e_i} = \kappa_i = 0$, $\varepsilon = 0.05$; $\sigma_{e_i} = \varepsilon = 0, \kappa_i = 0.05$ and $\kappa_i = \varepsilon = 0$, $\sigma_{e_i} = 0.05$. As can be seen from FIGURE 4, when either RHIs or ipSIC is existed, the outage performance of the system improves with the increase of SNR while if only CEEs appear in the system, there exists an error floor for the outage probability. The results show that the impact of CEEs on system performance is more serious than that of RHIs or ipSIC.

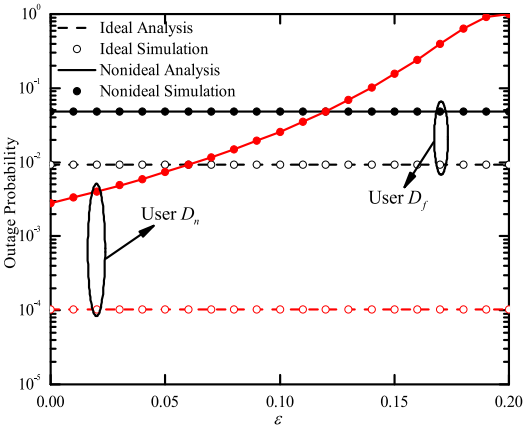

FIGURE 5. Outage probability of users versus ε in different conditions.

FIGURE 5 illustrates the impact of the ipSIC parameter on the system performance when SNR $= 20$dB. For D_f, we can see that the outage probability is always constant whether for

the ideal or non-ideal conditions which is due to that SIC has no effect on the far users, which is determined by the definition of SIC. For D_n, when the system is in the ideal conditions, the outage probability of the considered system is independent of the ipSIC parameter, thus the image of the outage probability is a parallel line. When the system is in the non-ideal conditions, the outage performance deteriorates with the ipSIC parameter increasing before $\varepsilon < 0.2$. From FIGURE 5, we can see that when $\varepsilon = 0.2$, the outage probability is close to 1, which is due to the conditions $a_2 > \left(\kappa^2_{SD_n} + a_1\varepsilon\right)\gamma_{thn}$ and $a_2 > (a_1 + d_2)\,\varepsilon\gamma_{thn}$ that are mentioned in Section 3 are not satisfied.

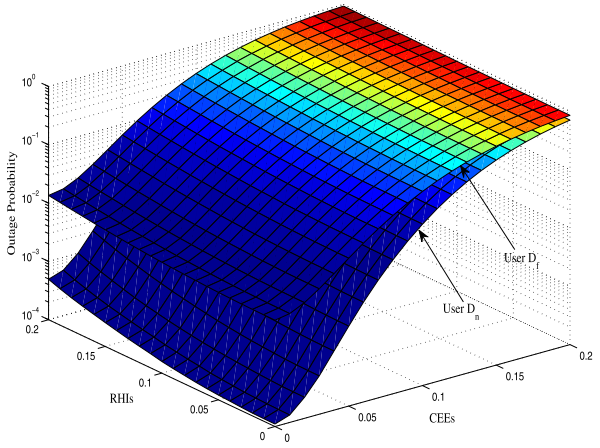

FIGURE 6. Outage probability of users versus κ and σ_e.

FIGURE 6 depicts the outage probability of the far users and the near users versus RHIs and CEEs with SNR = 20dB. The outage probability image of D_f is above D_n due to the large power allocation. From FIGURE 6, we can see that whether D_f or D_n, for a certain σ_e, when κ linearly increases from 0 to 0.2, the change of the outage probability is less pronounced. When σ_e increases from 0 to 0.2, for a certain κ, the change of outage probability of D_f and D_n is very obvious. This phenomenon indicates that the system performance is more sensitive to CEEs than RHIs on the other hand.

FIGURE 7 investigates ergodic sum rate of the users versus the transmit SNR both in ideal and non-ideal conditions. It is noticed from FIGURE 7 that in the non-ideal conditions, when SNR > 30dB, the ergodic rate tends to be constant, due to the presence of CEEs; in the ideal conditions, the ergodic rate of the near users increases with the increase of SNR while the far users tends to be stable. This happens because when $\gamma \to \infty$, the SINR of the near users is close to infinity, while tends to the fixed value a_1/a_2 for the far users. From another point of view, the results show that it is unreliable to improve system performance by simply improving SNR.

FIGURE 8 shows that the energy efficiency of the considered system versus transmit SNR in the ideal and non-ideal conditions. As can be observed from FIGURE 8, the energy efficiency is almost completely coincident and very negligible in the both ideal and non-ideal conditions when the SNR

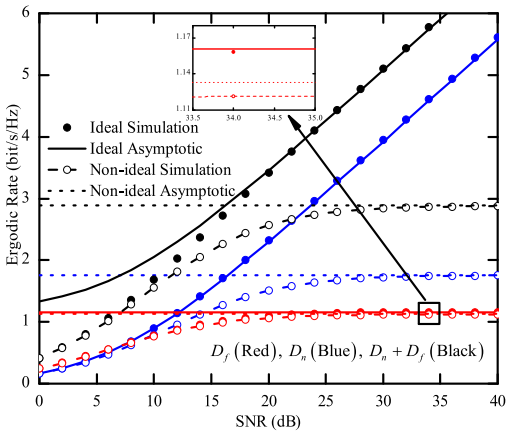

FIGURE 7. Ergodic sum rate versus SNR in different conditions.

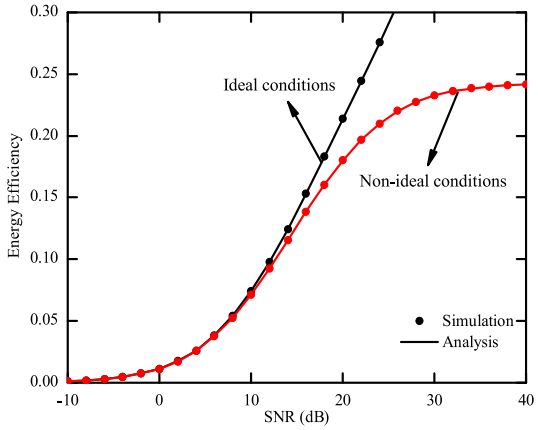

FIGURE 8. Energy efficiency versus SNR for different conditions.

is lower than 10dB, while with the SNR increasing, the gap of energy efficiency between ideal and non-ideal conditions becomes large. This situation is closely related to the outage probability. In the non-ideal conditions, when the system is in the high SNR region, there is an upper bound for the energy efficiency, which is the result of the joint action of RHIs, CEEs, and ipSIC.

VII. CONCLUSION

In this paper, we investigate the impact of NOMA AF relaying networks under the influence of RHIs, CEEs and ipSIC. The exact and asymptotic outage probability expressions are derived. Furthermore, the ergodic sum rate and the energy efficiency are also investigated. It is shown that RHIs, CEEs, and ipSIC all have a significant negative impact on system performance. In particular, we can observe that the effect of CEEs on the considered system outage performance is more obvious than that of RHIs. It can also be seen that the ergodic sum rate and energy efficiency have upper bounds, which means that the system performance will not be improved with the increase of SNR due to the existence of non-ideal factors.

APPENDIX A
PROOF OF THEOREM 1

Substituting (13) and (14) into (17), the outage probability of D_f can be rewritten as

$$\begin{aligned}&\mathrm{P}_{out}^{D_f}\\&=\underbrace{\Pr\left(\frac{a_1\rho_{SD_f}\gamma}{\left(a_2+\kappa_{SD_f}^2\right)\rho_{SD_f}\gamma+\left(\kappa_{SD_f}^2+1\right)\sigma_{e_{SD_f}}^2\gamma+1}\le\gamma_{thf}\right)}_{I_1}\\&\times\underbrace{\left[1-\Pr\left(\frac{\rho_{SR}\rho_{RD_f}a_1\gamma\gamma'}{\rho_{SR}\rho_{RD_f}(a_2+d_1)\gamma\gamma'+\rho_{RD_f}\gamma'\varphi_2+\rho_{SR}\gamma\varphi_1+\varphi_3}\ge\gamma_{thf}\right)\right]}_{I_2}.\end{aligned}\tag{A.1}$$

I_1 and I_2 are calculated as follows:

$$\begin{aligned}&I_1\\&=\Pr\left(\rho_{SD_f}<\frac{(\kappa_{SD_f}^2+1)\sigma_{e_5}^2\gamma\gamma_{thf}+\gamma_{thf}}{a_1\gamma-\left(a_2+\kappa_5^2\right)\gamma\gamma_{thf}}\triangleq\theta_2\right)\\&=b_f\sum_{z=0}^{M-f}\binom{M-f}{z}\frac{(-1)^z}{f+z}\left[1-\sum_{g_5=0}^{\alpha_{SD_f}-1}\frac{e^{-\frac{\theta_2}{\beta_{SD_f}}}}{g_5!}\left(\frac{\theta_2}{\beta_{SD_f}}\right)^{g_5}\right]^{f+z},\end{aligned}\tag{A.2}$$

$$\begin{aligned}&I_2\\&=1-\Pr\left(\frac{\rho_{SR}\rho_{RD_f}a_1\gamma\gamma'}{\rho_{SR}\rho_{RD_f}(a_2+d_1)\gamma\gamma'+\rho_{RD_f}\gamma'\varphi_2+\rho_{SR}\gamma\varphi_1+\varphi_3}\ge\gamma_{thf}\right)\\&=1-\Pr\left(\rho_{SR}\ge\theta_1,\rho_{RD_f}\ge\frac{(\rho_{SR}\gamma\varphi_1+\varphi_3)\theta_1}{(\rho_{SR}-\theta_1)\gamma'\varphi_2}\right)\\&=1-\int_{\theta_1}^{\infty}f_{\rho_{SR}}(y)\,dy\int_{\frac{(y\gamma\varphi_1+\varphi_3)\theta_1}{(y-\theta_1)\gamma'\varphi_2}}^{\infty}f_{\rho_{RD_f}}(x)dx\\&=1-\frac{2}{\Gamma(\alpha_{SR})\beta_{SR}^{\alpha_{SR}}}e^{-\frac{\theta_1}{\beta_{SR}}-\frac{\gamma\varphi_1\theta_1}{\beta_{RD_f}\gamma'\varphi_2}}\sum_{g_2=0}^{\alpha_{RD_f}-1}\frac{1}{g_2!}\sum_{u=0}^{\alpha_{SR}-1}\binom{\alpha_{SR}-1}{u}\\&\times\sum_{q=0}^{g_2}\binom{g_2}{q}\theta_1^{\alpha_{SR}+g_2-\frac{u+q+1}{2}}\left(\frac{1}{\beta_{RD_f}\gamma'\varphi_2}\right)^{g_2+\frac{u-q+1}{2}}(\gamma\varphi_1)^{g_2-q}\\&\times(\theta_1\gamma\varphi_1+\varphi_3)^{\frac{u+q+1}{2}}\beta_{SR}^{\frac{u-q+1}{2}}K_{u-q+1}\left(2\sqrt{\frac{\theta_1(\theta_1\gamma\varphi_1+\varphi_3)}{\beta_{SR}\beta_{RD_f}\gamma'\varphi_2}}\right).\end{aligned}\tag{A.3}$$

Combining (A.2) and (A.3), we can end the proof.

APPENDIX B
PROOF OF THEOREM 2

Substituting (11), (12), (15) and (16) into (19), the outage probability of D_n can be written as

$$\mathrm{P}_{out}^{D_n}=I_3\times I_4,\tag{B.1}$$

where I_3 and I_4 can be further expressed as

$$\begin{aligned}&I_3=1-\Pr\left(\rho_{SR}>\lambda_1,\rho_{RD_n}>\frac{(\rho_{SR}\gamma\varphi_5+\varphi_6)\lambda_1}{(\rho_{SR}-\lambda_1)\gamma'\varphi_4};\right.\\&\left.\rho_{SR}>\lambda_2,\rho_{RD_n}>\frac{(\rho_{SR}\gamma\varphi_5+\varphi_6)\lambda_2}{(\rho_{SR}-\lambda_2)\gamma'\varphi_4}\right)\\&=1-\Pr\left(\rho_{SR}>\lambda,\rho_{RD_n}>\frac{(\rho_{SR}\gamma\varphi_5+\varphi_6)\lambda}{(\rho_{SR}-\lambda)\gamma'\varphi_4}\right)\\&=1-\int_{\lambda}^{\infty}f_{\rho_{SR}}(y)\,dy\int_{\frac{(y\gamma\varphi_5+\varphi_6)\lambda}{(y-\lambda)\gamma'\varphi_4}}^{\infty}f_{\rho_{RD_n}}(x)dx\\&=1-\frac{2}{\Gamma(\alpha_{SR})\beta_{SR}^{\alpha_{SR}}}\sum_{g_3=0}^{\alpha_{RD_n}-1}\frac{1}{g_3!}\sum_{v=0}^{\alpha_{SR}-1}\binom{\alpha_{SR}-1}{v}\\&\times\sum_{t=0}^{g_3}\binom{g_3}{t}(\lambda\gamma\varphi_5+\varphi_6)^{\frac{v+t+1}{2}}\beta_{SR}^{\frac{v-t+1}{2}}e^{-\frac{\lambda}{\beta_{SR}}-\frac{\lambda\gamma\varphi_5}{\beta_{RD_n}\gamma'\varphi_4}}\\&\times\left(\frac{1}{\beta_{RD_n}\gamma'\varphi_4}\right)^{g_3+\frac{v-t+1}{2}}(\gamma\varphi_5)^{g_3-t}\lambda^{g_3+\alpha_{SR}-\frac{v+t+1}{2}}\\&\times K_{v-t+1}\left(2\sqrt{\frac{\lambda(\lambda\gamma\varphi_5+\varphi_6)}{\beta_{SR}\beta_{RD_n}\gamma'\varphi_4}}\right),\end{aligned}\tag{B.2}$$

$$\begin{aligned}&I_4=1-\Pr\left(\rho_{SD_n}>\tau_1,\rho_{SD_n}>\tau_2\right)\\&=1-\Pr(\rho_{SD_n}>\max(\tau_1,\tau_2)\triangleq\tau)\\&=b_n\sum_{z=0}^{M-n}\binom{M-n}{z}\frac{(-1)^z}{n+z}\left[1-\sum_{g_4=0}^{\alpha_{SD_n}-1}\frac{e^{-\frac{\tau}{\beta_{RD_n}}}}{g_4!}\left(\frac{\tau}{\beta_{SD_n}}\right)^{g_4}\right]^{n+z}.\end{aligned}\tag{B.3}$$

The reasoning processes of I_3 and I_4 are similar to that of I_1 and I_2. After some mathematical calculations, we can obtain (20).

APPENDIX C
PROOF OF COROLLARY 1

Based on (17), the asymptotic expression of outage probability of D_f in the ideal conditions can be expressed as

$$\mathrm{P}_{D_f}^{\infty,id}=\underbrace{\Pr\left(\rho_{SD_f}<\theta_2\right)}_{I_1^{\infty}}\underbrace{\left[1-\Pr\left(\frac{\rho_{SR}\rho_{RD_f}\gamma\gamma'}{\rho_{SR}\gamma\varphi_1+\rho_{RD_f}\gamma'\varphi_2+\varphi_3}>b_1\right)\right]}_{I_2^{\infty}}.\tag{C.1}$$

Using the inequality $xy/(1+x+y)<\min(x,y)$, I_2^{∞} can be rewritten as

$$\begin{aligned}I_2^{\infty}&=1-\Pr\left(\min\left(\frac{\rho_{SR}\gamma\varphi_1}{\varphi_3},\frac{\rho_{RD_f}\gamma'\varphi_2}{\varphi_3}\right)>\frac{b_1\varphi_1\varphi_2}{\varphi_3}\right)\\&\approx F_{\rho_{SR}}^{\infty}\left(\frac{\varphi_2 b_1}{\gamma}\right)+F_{\rho_{RD_f}}^{\infty}\left(\frac{\varphi_1 b_1}{\gamma'}\right).\end{aligned}\tag{C.2}$$

Substituting (C.4) into (C.1), using (21) and (22), after some mathematical calculations, we can obtain (23).

$$P_{D_n}^{\infty,id} = \underbrace{\Pr\left(\rho_{SD_n} < \tau\right)}_{I_4^\infty} \times \underbrace{\left[1 - \Pr\left(\frac{\rho_{SR}\rho_{RD_n}\gamma\gamma'}{\rho_{RD_n}\gamma'\varphi_4 + \rho_{SR}\gamma\varphi_5 + \varphi_6} > b_2, \frac{\rho_{SR}\rho_{RD_n}\gamma\gamma'}{\rho_{RD_n}\gamma'\varphi_4 + \rho_{SR}\gamma\varphi_5 + \varphi_6} > b_3\right)\right]}_{I_3^\infty} \tag{D.1}$$

In the non-ideal conditions, I_1^∞ and I_2^∞ can be expressed as

$$I_1^\infty = \Pr\left(\rho_{SD_f} < \theta_2'\right), \tag{C.3}$$

$$I_2^\infty = 1 - \Pr\left(\rho_{SR} \geq \theta_1', \rho_{RD_f} \geq \frac{\left(\rho_{SR} + \sigma_{e_{SR}}^2\right)\theta_1'\sigma_{e_{RD_f}}^2}{\left(\rho_{SR} - \theta_1'\right)\sigma_{e_{SR}}^2}\right). \tag{C.4}$$

Substituting (10) into (C.3) and substituting (8), (10) into (C.4), after some mathematical calculations, we can obtain (24).

APPENDIX D
PROOF OF COROLLARY 2

Substituting (11), (12), (15) and (16) into (19), the asymptotic expression of outage probability of D_n in the ideal conditions is given at the top of this page.

Using the inequality $xy/(1+x+y) < \min(x, y)$ [45], I_3^∞ can be rewritten as

$$\begin{aligned} I_3^\infty &= 1 - \Pr\left(\min\left(\frac{\rho_{SR}\gamma\varphi_5}{\varphi_6}, \frac{\rho_{RD_n}\gamma'\varphi_4}{\varphi_6}\right) > \frac{\varphi_4\varphi_5 b_2}{\varphi_6}, \right. \\ &\quad \left. \min\left(\frac{\rho_{SR}\gamma\varphi_5}{\varphi_6}, \frac{\rho_{RD_n}\gamma'\varphi_4}{\varphi_6}\right) > \frac{\varphi_4\varphi_5 b_3}{\varphi_6}\right) \\ &= 1 - \Pr\left(\rho_{SR} > \psi, \rho_{RD_n} > \xi\right) \\ &\approx F_{\rho_{SR}}^\infty(\psi) + F_{\rho_{RD_n}}^\infty(\xi). \end{aligned} \tag{D.2}$$

Substituting (D.2) into (D.1), using (21) and (22), after some mathematical calculations, we can obtain (25).

In the non-ideal conditions, I_3^∞ and I_4^∞ can be expressed as

$$\begin{aligned} I_3^\infty &= 1 - \Pr\left(\rho_{SR} > \lambda'_1, \rho_{RD_n} > \frac{\left(\rho_{SR} + \sigma_{e_{SR}}^2\right)\sigma_{e_{RD_n}}^2\lambda'_1}{\left(\rho_{SR} - \lambda'_1\right)\sigma_{e_{SR}}^2}; \right. \\ &\quad \left. \rho_{SR} > \lambda'_2, \rho_{RD_n} > \frac{\left(\rho_{SR} + \sigma_{e_{SR}}^2\right)\sigma_{e_{RD_n}}^2\lambda'_2}{\left(\rho_{SR} - \lambda'_2\right)\sigma_{e_{SR}}^2}\right) \\ &= 1 - \Pr\left(\rho_{SR} > \lambda', \rho_{RD_n} > \frac{\left(\rho_{SR} + \sigma_{e_{SR}}^2\right)\sigma_{e_{RD_n}}^2\lambda'}{\left(\rho_{SR} - \lambda'\right)\sigma_{e_{SR}}^2}\right), \end{aligned} \tag{D.3}$$

$$\begin{aligned} I_4^\infty &= 1 - \Pr\left(\rho_{SD_n} > \tau_1', \rho_{SD_n} > \tau_2'\right) \\ &= 1 - \Pr\left(\rho_{SD_n} > \tau'\right). \end{aligned} \tag{D.4}$$

Substituting (7), (8) into (D.3) and substituting (10) into (D.4), after some mathematical calculations, we can obtain (26).

APPENDIX E

Substituting (13) and (14) into (27), the ergodic rate of D_f in the non-ideal conditions can be expressed as

$$\begin{aligned} R_{ave}^{f,nid} &= \mathbb{E}\left[\frac{1}{2}\log_2\left(1 + \max\left[\frac{a_1\rho_{SD_f}\gamma}{\left(a_2 + \kappa_{SD_f}^2\right)\rho_{SD_f}\gamma + \left(\kappa_{SD_f}^2 + 1\right)\sigma_{e_{SD_f}}^2\gamma + 1}, \right.\right.\right. \\ &\quad \left.\left.\left. \frac{\rho_{SR}\rho_{RD_f}a_1\gamma\gamma'}{\rho_{SR}\rho_{RD_f}\left(a_2 + d_1\right)\gamma\gamma' + \rho_{RD_f}\gamma'\varphi_2 + \rho_{SR}\gamma\varphi_1 + \varphi_3}\right]\right)\right]. \end{aligned} \tag{E.1}$$

Following the inequality [46]

$$\mathbb{E}\left[\log_2\left(1 + \frac{x}{y}\right)\right] \approx \log_2\left(1 + \frac{\mathbb{E}(x)}{\mathbb{E}(y)}\right) \tag{E.2}$$

(E.1) can be rewritten as

$$\begin{aligned} R_{ave}^{f,nid} &= \frac{1}{2}\log_2\left(1 + \max\left[\right.\right. \\ &\quad \frac{a_1\mathbb{E}\left[\rho_{SD_f}\right]\gamma}{\left(a_2 + \kappa_{SD_f}^2\right)\mathbb{E}\left[\rho_{SD_f}\right]\gamma + \left(\kappa_{SD_f}^2 + 1\right)\sigma_{e_{SD_f}}^2\gamma + 1}, \\ &\quad \left.\left. \frac{\mathbb{E}[\rho_{SR}]\mathbb{E}\left[\rho_{RD_f}\right]a_1\gamma\gamma'}{\mathbb{E}[\rho_{SR}]\mathbb{E}\left[\rho_{RD_f}\right](a_2+d_1)\gamma\gamma' + \mathbb{E}\left[\rho_{RD_f}\right]\gamma'\varphi_2 + \mathbb{E}[\rho_{SR}]\gamma\varphi_1 + \varphi_3}\right]\right). \end{aligned} \tag{E.3}$$

Defining $\Lambda_1 \triangleq \mathbb{E}[\rho_{SR}]$, $\Lambda_2 = \mathbb{E}\left[\rho_{RD_n}\right]$ and using [47, Eq. 3.478.1], therefore Λ_1 and Λ_2 can be expressed as

$$\begin{aligned} \Lambda_1 &= \int_0^\infty x f_{\rho_{SR}}(x)dx \\ &= \int_0^\infty \frac{x^{\alpha_{SR}}}{\Gamma(\alpha_{SR})\beta_{SR}^{\alpha_{SR}}} e^{-\frac{x}{\beta_{SR}}} dx \\ &= (\alpha_{SR} + 1)\beta_{SR}, \end{aligned} \tag{E.4}$$

$$\begin{aligned} \Lambda_2 &= \int_0^\infty x f_{\rho_{RD_f}}(x)dx \\ &= \int_0^\infty \frac{b_f x^{\alpha_{RD_f}}}{\Gamma(\alpha_{RD_f})\beta_{RD_f}^{\alpha_{RD_f}}} \left[1 - \sum_{g_2=0}^{\alpha_{RD_f}-1} \frac{e^{-\frac{x}{\beta_{RD_f}}}}{g_2!}\left(\frac{x}{\beta_{RD_f}}\right)^{g_2}\right]^{f-1} \\ &\quad \times e^{-\frac{x}{\beta_{RD_f}}} \left[\sum_{g_2=0}^{\alpha_{RD_f}-1} \frac{e^{-\frac{x}{\beta_{RD_f}}}}{g_2!}\left(\frac{x}{\beta_{RD_f}}\right)^{g_2}\right]^{M-f} dx \end{aligned}$$

$$= \frac{b_f \Gamma(c_2)}{\Gamma(\alpha_{RD_f}) \beta_{RD_f}^{\alpha_{RD_f}}} \sum_{t=0}^{f-1} \binom{f-1}{t} (-1)^t \sum_{p_0+\cdots+p_{\alpha_{RD_f}-1}=c_1} \times \binom{c_1}{p_0, \cdots, p_{\alpha_{RD_f}-1}} \prod_{g_2=0}^{\alpha_{RD_f}-1} \left(\frac{1}{g_2!}\right)^{p_{g_2}} \left(\frac{1}{\beta_{RD_f}}\right)^{g_2 p_{g_2}} \left(\frac{c_1+1}{\beta_{RD_f}}\right)^{-c_2}, \tag{E.5}$$

Similarly, we can obtain Λ_3, Λ_4, and Λ_5 in the same way, respectively. Substituting Λ_1, Λ_2 and Λ_5 into (E.3), we can obtain (31).

APPENDIX F

Substituting (12) and (16) into (28), and using the inequality $xy/(1+x+y) < \min(x, y)$, we can obtain

$$\begin{aligned} R_{ave}^{n_1,id} &= \mathbb{E}\left[\frac{1}{2\ln 2} \ln\left(1 + \max\left[\gamma_{SD_n}, \gamma_{RD_n}\right]\right)\right] \\ &< \frac{1}{2\ln 2} \mathbb{E}\left\{\ln\left(1 + a_2 \max\left[\rho_{SD_n}\gamma, \min\left(\rho_{SR}\gamma, \rho_{RD_n}\gamma'\right)\right]\right)\right\}. \end{aligned} \tag{F.1}$$

Denote $W = \max\left[\rho_{SD_n}\gamma, \min\left(\rho_{SR}\gamma, \rho_{RD_n}\gamma'\right)\right]$, according to the knowledge of probability theory, we can get

$$\begin{aligned} F_W(w) &= \Pr\left(\max\left[\rho_{SD_n}\gamma, \min\left(\rho_{SR}\gamma, \rho_{RD_n}\gamma'\right)\right] \le w\right) \\ &= \Pr\left(\rho_{SD_n}\gamma \le w\right)\left[1 - \Pr\left(\rho_{SR} > \frac{w}{\gamma}\right)\Pr\left(\rho_{RD_n} > \frac{w}{\gamma'}\right)\right] \\ &= b_n \sum_{z=0}^{M-n} \binom{M-n}{z} \frac{(-1)^z}{n+z} \left[1 - \sum_{g_4=0}^{\alpha_{SD_n}-1} \frac{e^{-\frac{w}{\beta_{SD_n}\gamma}}}{g_4!} \times \left(\frac{w}{\beta_{SD_n}\gamma}\right)^{g_4}\right]^{M-n} \left[1 - \sum_{g_1=0}^{\alpha_{SR}-1} \sum_{g_3=0}^{\alpha_{RD_n}-1} \frac{1}{g_1! g_3!} \left(\frac{1}{\beta_{SD_n}\gamma}\right)^{g_1} \times e^{-\frac{w}{\beta_{SD_n}\gamma} - \frac{w}{\beta_{RD_n}\gamma'}} \left(\frac{1}{\beta_{RD_n}\gamma'}\right)^{g_3} w^{g_1+g_3}\right]. \end{aligned} \tag{F.2}$$

Base on (F.3) and (F.2), $R_{ave}^{n,1}$ can be rewritten as

$$\begin{aligned} R_{ave}^{n_1,id} &< \frac{1}{2\ln 2} \mathbb{E}\{\ln(1+a_2 w)\} \\ &= \frac{1}{2\ln 2} \int_0^\infty f_W(w) \ln(1+a_2 w) dw \\ &= \frac{a_2}{2\ln 2} \int_0^\infty \frac{1 - F_W(w)}{1+a_2 w} dw \\ &= \frac{a_2 b_n}{2\ln 2} \sum_{z=0}^{M-n} \binom{M-n}{z} \frac{(-1)^z}{n+z} (\Phi_1 + \Phi_2 - \Phi_3). \end{aligned} \tag{F.3}$$

In the above formula, Φ_1, Φ_2 and Φ_3 can be expressed as

$$\Phi_1 = \sum_{g_1=0}^{\alpha_{SR}-1} \sum_{g_3=0}^{\alpha_{RD_n}-1} \vartheta \int_0^\infty \frac{e^{-\frac{w}{\beta_{SR}\gamma} - \frac{w}{\beta_{RD_n}\gamma'}} w^{g_1+g_3}}{1+a_2 w} dw, \tag{F.4}$$

$$\Phi_2 = \sum_{g_1=0}^{\alpha_{SR}-1} \sum_{g_3=0}^{\alpha_{RD_n}-1} \sum_{q=1}^{M-n} \binom{M-n}{q} (-1)^q \vartheta \times \int_0^\infty \frac{\left[\sum_{g_4=0}^{\alpha_{SD_n}-1} \frac{1}{g_4!} e^{-\frac{w}{\beta_{SD_n}\gamma}} \left(\frac{w}{\beta_{SD_n}\gamma}\right)^{g_4}\right]^q e^{-\frac{w}{\beta_{SR}\gamma} - \frac{w}{\beta_{RD_n}\gamma'}} w^{g_1+g_3}}{1+a_2 w} dw, \tag{F.5}$$

$$\Phi_3 = \sum_{q=1}^{M-n} \binom{M-n}{q} (-1)^q \times \int_0^\infty \frac{\left(\sum_{g_4=0}^{\alpha_{SD_n}-1} \frac{1}{g_4!} e^{-\frac{w}{\beta_{SD_n}\gamma}} \left(\frac{w}{\beta_{SD_n}\gamma}\right)^{g_4}\right)^q}{1+a_2 w} dw, \tag{F.6}$$

where $\vartheta = (g_1! g_3!)^{-1} (\beta_{SR}\gamma)^{-g_1} \left(\beta_{RD_n}\gamma'\right)^{-g_3}$. With the aid of [47, Eq. 3.352.4] and [47, Eq. 3.353.5], after some mathematical calculations, we can obtain the final representation

$$\Phi_1 = \begin{cases} -\frac{1}{a_2} \sum_{g_1=0}^{\alpha_{SR}-1} \sum_{g_3=0}^{\alpha_{RD_n}-1} \vartheta e^{f_1+f_3} \mathrm{Ei}(-f_1-f_3), & l_1 = 0 \\ \sum_{g_1=0}^{\alpha_{SR}-1} \sum_{g_3=0}^{\alpha_{RD_n}-1} \left(\frac{1}{a_2}\right)^{l_1+1} \vartheta \left[(-1)^{l_1-1} e^{f_1+f_3} \mathrm{Ei}(-f_1-f_3) + \sum_{L=1}^{l_1} (L-1)!(-1)^{l_1-L} (f_1+f_3)^{-L}\right], & l_1 > 0, \end{cases} \tag{F.7}$$

$$\Phi_2 = \begin{cases} -\Xi_1 e^{f_1+f_2+qf_3} \mathrm{Ei}(-f_1-f_2-qf_3), & l_2 = 0 \\ \Xi_1 \left[(-1)^{l_2-1} e^{f_1+f_2+qf_3} \mathrm{Ei}(-f_1-f_2-qf_3) + \sum_{L=1}^{l_2} (L-1)!(-1)^{l_2-L} (f_1+f_2+qf_3)^{-L}\right], & l_2 > 0, \end{cases} \tag{F.8}$$

$$\Phi_3 = \begin{cases} -\Xi_2 e^{f_3} \mathrm{Ei}(-f_3), & g_4 p_{g_4} = 0 \\ \Xi_2 \left[(-1)^{g_4 p_{g_4}-1} e^{f_3} \mathrm{Ei}(-f_3) + \sum_{L=1}^{g_4 p_{g_4}} (L-1)!(-1)^{g_4 p_{g_4}-L} f_3^{-L}\right], & g_4 p_{g_4} > 0, \end{cases} \tag{F.9}$$

where $f_1 = (a_2 \beta_{SR}\gamma)^{-1}$, $f_2 = \left(a_2 \beta_{RD_n}\gamma'\right)^{-1}$, $f_3 = \left(a_2 \beta_{SD_n}\gamma\right)^{-1}$, $l_1 = g_1 + g_3$, $l_2 = g_1 + g_3 + g_4 p_{g_4}$, and $\mathrm{Ei}(\cdot)$ denotes the exponential integral functions. Ξ_1 and Ξ_2

are expressed as

$$\Xi_1 = \sum_{g_1=0}^{\alpha_{SR}-1}\sum_{g_3=0}^{RD_n-1}\sum_{q=1}^{M-n}\binom{M-n}{q}(-1)^q\vartheta\left(\frac{1}{a_2}\right)^{l_2+1} \times \sum_{p_0+\cdots+p_{\alpha_{SD_n}-1}=q}\binom{q}{p_0,\cdots,p_{\alpha_{SD_n}-1}}\prod_{g_4=0}^{\alpha_{SD_n}-1}\left(\frac{1}{g_4!}\right)^{p_{g_4}}, \tag{F.10}$$

$$\Xi_2 = \frac{1}{a_2}\sum_{q=1}^{M-n}\binom{M-n}{q}(-1)^q f_3^{g_4p_{g_4}} \times \sum_{p_0+\cdots+p_{\alpha_{SD_n}-1}=q}\binom{q}{p_0,\cdots,p_{\alpha_{SD_n}-1}}\prod_{g_4=0}^{\alpha_{SD_n}-1}\left(\frac{1}{g_4!}\right)^{p_{g_4}}. \tag{F.11}$$

Substituting (F.7)-(F.11) into (F.3), we can obtain $R_{ave}^{n_1,id}$.

Similarly, $R_{ave}^{n_2,id}$ can be expressed as follows

$$\begin{aligned} R_{ave}^{n_2,id} &= \mathbb{E}\left[\frac{1}{2}\log_2\left(1+a_2\rho_{SD_n}\gamma\right)\right] \\ &= \frac{a_2\gamma}{2\ln 2}\int_0^\infty \frac{1-F_{\rho_{SD_n}}(x)}{1+a_2\gamma x}dx \\ &= -\frac{b_n}{2\ln 2}\sum_{z=0}^{M-n}\binom{M-n}{z}\frac{(-1)^z}{n+z}\Phi_4. \end{aligned} \tag{F.12}$$

Following [47, Eq. 3.352.4] and [47, Eq. 3.353.5], Φ_4 can be further expressed as

$$\Phi_4 = \begin{cases} -e^{tf_3}\mathrm{Ei}\left(-tf_3\right), g_4p_{g_4}=0 \\ \sum_{L=1}^{g_4p_{g_4}}(L-1)!(-1)^{g_4p_{g_4}-L}(tf_3)^{-L} \\ +(-1)^{g_4p_{g_4}-1}e^{tf_3}\mathrm{Ei}\left(-tf_3\right), g_4p_{g_4}>0. \end{cases} \tag{F.13}$$

Ξ_3 is expressed as

$$\Xi_3 = \sum_{t=1}^{n+z}(-1)^t\sum_{p_0+\cdots+p_{\alpha_{SD_n}-1}=t}\binom{t}{p_0,\cdots,p_{\alpha_{SD_n}-1}} \times \prod_{g_4=0}^{\alpha_{SD_n}-1}\left(\frac{1}{g_4}\right)^{p_{g_4}}f_3^{g_4p_{g_4}}. \tag{F.14}$$

Combining the above formulas, we can end the proof.

REFERENCES

[1] H. Wang, Z. Zhang, and X. Chen, "Energy-efficient power allocation for non-orthogonal multiple access with imperfect successive interference cancellation," in *Proc. 9th Int. Conf. Wireless Commun. Signal Process.*, Oct. 2017, pp. 1–6.

[2] U. Varshney, "4G wireless networks," *IT Prof.*, vol. 14, no. 5, pp. 34–39, Sep./Oct. 2012.

[3] D. Zhang, Y. Liu, L. Dai, A. K. Bashir, A. Nallanathan, and B. Shim, "Performance analysis of FD-NOMA-based decentralized V2X systems," *IEEE Trans. Commun.*, vol. 67, no. 7, pp. 5024–5036, Jul. 2019.

[4] T M. C. Thomas and A. T. Joy, *Elements of Information Theory*, 2nd ed. New York, NY, USA: Springer, 2006.

[5] M. Kontik and S. C. Ergen, "Scheduling in successive interference cancellation based wireless ad hoc networks," *IEEE Commun. Lett.*, vol. 19, no. 9, pp. 1524–1527, Sep. 2015.

[6] X. Li, M. Liu, D. Deng, J. Li, C. Deng, and Q. Yu, "Power beacon assisted wireless power cooperative relaying using NOMA with hardware impairments and imperfect CSI," *AEU-Int. J. Electron. Commun.*, vol. 108, pp. 275–286, Aug. 2019.

[7] Z. Wei, J. Guo, D. W. K. Ng, and J. Yuan, "Fairness comparison of uplink NOMA and OMA," in *Proc. IEEE 85th Veh. Technol. Conf.*, Jun. 2017, pp. 1–6.

[8] Y. Liu, Z. Ding, M. Elkashlan, and H. V. Poor, "Cooperative non-orthogonal multiple access with simultaneous wireless information and power transfer," *IEEE J. Sel. Areas Commun.*, vol. 34, no. 4, pp. 938–953, Apr. 2016.

[9] T. Do, D. B. Da Costa, T. Q. Duong, and B. An, "Improving the performance of cell-edge users in NOMA systems using cooperative relaying," *IEEE Trans. Commun.*, vol. 66, no. 5, pp. 1883–1901, May 2018.

[10] Z. Ding, M. Peng, and H. V. Poor, "Cooperative non-orthogonal multiple access in 5G systems," *IEEE Commun. Lett.*, vol. 19, no. 8, pp. 1462–1465, Aug. 2015.

[11] X. Li, M. Liu, C. Deng, P. T. Mathiopoulos, Z. Ding, and Y. Liu, "Full-duplex cooperative NOMA relaying systems with I/Q imbalance and imperfect SIC," *IEEE Wireless Commun. Lett.*, to be published.

[12] M. R. Usman, A. Khan, M. A. Usman, J. Y. Seong, and S. Y. Shin, "On the performance of perfect and imperfect SIC in downlink non orthogonal multiple access (NOMA)," in *Proc. Int. Conf. Smart Green Technol. Elect. Inf. Syst.*, Oct. 2016, pp. 102–106.

[13] X. Yue, Z. Qin, Y. Liu, S. Kang, and Y. Chen, "A unified framework for non-orthogonal multiple access," *IEEE Trans. Commun.*, vol. 66, no. 11, pp. 5346–5359, Nov. 2018.

[14] Q. Wang, J. Ge, Q. Li, and Q. Bu, "Performance analysis of NOMA for multiple-antenna relaying networks with energy harvesting over Nakagami-m fading channels," in *Proc. IEEE/CIC Int. Conf. Commun. China*, Oct. 2017, pp. 1–5.

[15] Z. Qin, F. Y. Li, G. Y. Li, J. A. McCann, and Q. Ni, "Low-power wide-area networks for sustainable IoT," *IEEE Wireless Commun.*, vol. 26, no. 3, pp. 140–145, Jun. 2019.

[16] Y. Alsaba, C. Y. Leow, and S. K. A. Rahim, "Full-duplex cooperative non-orthogonal multiple access with beamforming and energy harvesting," *IEEE Access*, vol. 6, pp. 19726–19738, 2018.

[17] H.-S. Nguyen, T.-S. Nguyen, P. T. Tin, and M. Voznak, "Outage performance of time switching energy harvesting wireless sensor networks deploying NOMA," in *Proc. IEEE 20th Int. Conf. e-Health Netw., Appl. Services*, Sep. 2018, pp. 1–4.

[18] R. Zhang and C. K. Ho, "MIMO broadcasting for simultaneous wireless information and power transfer," *IEEE Trans. Wireless Commun.*, vol. 12, no. 5, pp. 1989–2001, May 2013.

[19] Y. Xu, C. Shen, Z. Ding, X. Sun, S. Yan, G. Zhu, and Z. Zhong, "Joint beamforming and power-splitting control in downlink cooperative SWIPT NOMA systems," *IEEE Trans. Signal Process.*, vol. 65, no. 18, pp. 4874–4886, Sep. 2017.

[20] T.-S. Nguyen, H. H. K. Duy, H.-S. Nguyen, and M. Voznak, "Throughput analysis in relaying cooperative systems considering time-switching with NOMA," in *Proc. 41st Int. Conf. Telecommun. Signal Process.*, Jul. 2018, pp. 1–4.

[21] X. Li, J. Li, Y. Liu, Z. Ding, and A. Nallanathan, "Outage performance of cooperative NOMA networks with hardware impairments," in *Proc. IEEE Global Commun. Conf.*, Dec. 2018, pp. 1–6.

[22] X. Li, M. Huang, C. Zhang, D. Deng, K. M. Rabie, Y. Ding, and J. Du, "Security and reliability performance analysis of cooperative multi-relay systems with nonlinear energy harvesters and hardware impairments," *IEEE Access*, vol. 7, pp. 102644–102661, 2019.

[23] V. Rampa, "I/Q compensation of broadband direct-conversion transmitters," *IEEE Trans. Wireless Commun.*, vol. 13, no. 6, pp. 3329–3342, Jun. 2014.

[24] L. Feng and W. Namgoong, "SPC09-4: A hardware impairment compensation scheme with cascaded adaptive filters," in *Proc. IEEE GLOBECOM*, Nov./Dec. 2006, pp. 1–6.

[25] S. Lajnef, N. Boulejfen, A. Abdelhafiz, and F. M. Ghannouchi, "Two-dimensional Cartesian memory polynomial model for nonlinearity and I/Q imperfection compensation in concurrent dual-band transmitters," *IEEE Trans. Circuits Syst. II, Exp. Brief*, vol. 63, no. 1, pp. 14–18, Jan. 2016.
[26] P. K. Sharma and P. K. Upadhyay, "Cognitive relaying with transceiver hardware impairments under interference constraints," *IEEE Commun. Lett.*, vol. 20, no. 4, pp. 820–823, Apr. 2016.
[27] F. Ding, H. Wang, S. Zhang, and M. Dai, "Impact of residual hardware impairments on non-orthogonal multiple access based amplify-and-forward relaying networks," *IEEE Access*, vol. 6, pp. 15117–15131, 2018.
[28] J. Cui, Z. Ding, and P. Fan, "Outage probability constrained MIMO-NOMA designs under imperfect CSI," *IEEE Trans. Wireless Commun.*, vol. 17, no. 12, pp. 8239–8255, Dec. 2018.
[29] X. Li, M. Matthaiou, Y. Liu, H. Q. Ngo, and L. Li, "Multi-pair two-way massive MIMO relaying with hardware impairments over Rician fading channels," in *Proc. IEEE Global Commun. Conf.*, Dec. 2018, pp. 1–6.
[30] S. Furrer and D. Dahlhaus, "Multiple-antenna signaling over fading channels with estimated channel state information: Capacity analysis," *IEEE Trans. Inf. Theory*, vol. 53, no. 6, pp. 2028–2043, Jun. 2007.
[31] S. Liu, Z. Liu, D. Sun, H. Yang, K. Yi, and K. Wang, "On the performance of wireless-powered cooperative DF relaying networks with imperfect CSI," *China Commun.*, vol. 15, no. 11, pp. 79–92, Nov. 2018.
[32] X. Tang, M.-S. Alouini, and A. J. Goldsmith, "Effect of channel estimation error on M-QAM BER performance in Rayleigh fading," *IEEE Trans. Commun.*, vol. 47, no. 12, pp. 1856–1864, Dec. 1999.
[33] A. K. Mishra, D. Mallick, and P. Singh, "Combined effect of RF impairment and CEE on the performance of dual-hop fixed-gain AF relaying," *IEEE Commun. Lett.*, vol. 20, no. 9, pp. 1725–1728, Sep. 2016.
[34] A. K. Mishra and P. Singh, "Performance analysis of opportunistic transmission in downlink cellular DF relay network with channel estimation error and RF impairments," *IEEE Trans. Veh. Technol.*, vol. 67, no. 9, pp. 9021–9026, Sep. 2018.
[35] J. Li, X. Li, Y. Liu, C. Zhang, L. Li, and A. Nallanathan, "Joint impact of hardware impairments and imperfect channel state information on multi-relay networks," *IEEE Access*, vol. 7, pp. 72358–72375, 2019.
[36] Y. Li, Y. Wang, and T. Jiang, "Norm-adaption penalized least mean square/fourth algorithm for sparse channel estimation," *Signal Process.*, vol. 128, pp. 243–251, 2016.
[37] M. Médard, "The effect upon channel capacity in wireless communications of perfect and imperfect knowledge of the channel," *IEEE Trans. Inf. Theory*, vol. 46, no. 3, pp. 933–946, May 2000.
[38] A. K. Mishra, D. Mallick, M. Issar, and P. Singh, "Performance analysis of dual-hop DF relaying systems in the combined presence of CEE and RFI," in *Proc. 9th Int. Conf. Commun. Syst. Netw.*, Jan. 2017, pp. 354–359.
[39] Y. Ma and J. Jin, "Effect of channel estimation errors on M -QAM with MRC and EGC in Nakagami fading channels," *IEEE Trans. Veh. Technol.*, vol. 56, no. 3, pp. 1239–1250, May 2007.
[40] T. Schenk, *RF Imperfections in High-Rate Wireless Systems: Impact and Digital Compensation*. New York, NY, USA: Springer, 2008.
[41] X. Li, J. Li, and L. Li, "Performance analysis of impaired SWIPT NOMA relaying networks over imperfect weibull channels," *IEEE Syst. J.*, to be published.
[42] G. Im and J. H. Lee, "Outage probability for cooperative NOMA systems with imperfect SIC in cognitive radio networks," *IEEE Commun. Lett.*, vol. 23, no. 4, pp. 692–695, Apr. 2019.
[43] J. Men, J. Ge, and C. Zhang, "Performance analysis of nonorthogonal multiple access for relaying networks over Nakagami-m fading channels," *IEEE Trans. Veh. Technol.*, vol. 66, no. 2, pp. 1200–1208, Feb. 2017.
[44] W. Yang, W. Mou, X. Xu, W. Yang, and Y. Cai, "Energy efficiency analysis and enhancement for secure transmission in SWIPT systems exploiting full duplex techniques," *IET Commun.*, vol. 10, no. 14, pp. 1712–1720, 2016.
[45] A. Bletsas, A. Khisti, D. P. Reed, and A. Lippman, "A simple cooperative diversity method based on network path selection," *IEEE J. Sel. Areas Commun.*, vol. 24, no. 3, pp. 659–672, Mar. 2006.
[46] E. Bjornson, M. Matthaiou, and M. Debbah, "A new look at dual-hop relaying: Performance limits with hardware impairments," *IEEE Trans. Commun.*, vol. 61, no. 11, pp. 4512–4525, Nov. 2013.
[47] I. S. Gradshteĭn and I. M. Ryžhik, *Table of Integrals, Series, and Products*, 7th ed. San Diego, CA, USA: Academic, 2007.

XINGWANG LI (S'12–M'15) received the B.Sc. degree in communication engineering from Henan Polytechnic University, Jiaozuo, China, in 2007, the M.Sc. degree from the National Key Laboratory of Science and Technology on Communications, University of Electronic Science and Technology of China (UESTC), in 2010, and the Ph.D. degree from the State Key Laboratory of Networking and Switching Technology, Beijing University of Posts and Telecommunications (BUPT), in 2015. From 2010 to 2012, he was an Engineer with Comba Telecom Ltd., Guangzhou, China. From 2017 to 2018, he was a Visiting Scholar with the Institute of Electronics, Communications and Information Technology (ECIT), Queen's University Belfast (QUB), Belfast, U.K. He is currently an Associate Professor with the School of Physics and Electronic Information Engineering, Henan Polytechnic University. He has several articles published in journal and conferences, authored several patents, and worked on several funded research projects on the wireless communications areas. His research interests include MIMO communication, cooperative communication, hardware constrained communication, non-orthogonal multiple access (NOMA), physical layer security, unmanned aerial vehicles (UAVs), free-space optical (FSO) communications, and performance analysis of fading channels. He has served as a TPC Member of the 2018 IEEE Globecom Workshop. He is also a TPC Member of the 2019 IEEE/CIC ICCC Workshop. He also serves as an Associate Editor for IEEE Access and the Technical Committee of *Computer Communications*. He is also an Editor of the *KSII Transactions on Internet and Information Systems*.

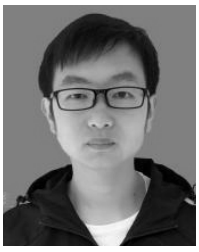

MENG LIU (S'19) received the B.Sc. degree in electronic information engineering from the School of Physics and Electronic Information Engineering, Henan Polytechnic University, Jiaozuo, China, in 2016, where he is currently pursuing the M.Sc. degree in communication and information systems. His current research interests include non-orthogonal multiple access (NOMA), and simultaneous wireless information and power transfer (SWIPT).

CHAO DENG received the B.Sc. and M. Sc. degrees in communication engineering from Jilin University, China, in 2002 and 2005, respectively, and the Ph.D. degree from the Changchun Institute of Optics, Fine Mechanics and Physics, Chinese Academy of Sciences, in 2008. He is currently an Associate Professor with the School of Physics and Electronic Information Engineering, Henan Polytechnic University, Jiaozuo, China. His research interests include wireless communication, image processing, and signal processing.

DI ZHANG (S'13–M'17) received the Ph.D. degree from Waseda University, Tokyo, Japan, in 2017. He visited the National Key Laboratory of Alternate Electrical Power System With Renewable Energy Sources, Beijing, China, from 2015 to 2017, and the National Chung Hsing University, Taichung, Taiwan, in 2012. He is currently an Assistant Professor with Zhengzhou University, Zhengzhou, China, and a Visiting Researcher with Seoul National University, Seoul, South Korea. His research interests include 5G wireless networks, the Internet of Things, and telemedicine. He has served as the Guest Editors of the IEEE NETWORK, IEEE ACCESS, the *IET Intelligent Transport Systems*, and a TPC Member for many IEEE flagship conferences, such as ICC and WCNC. He also serves as an Editor for the *KSII Transactions on Internet and Information Systems*.

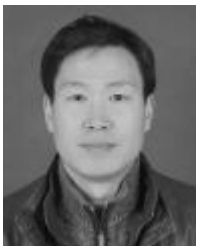

XIANG-CHUAN GAO received the B.Sc. and M.Eng. degrees from Zhengzhou University, Zhengzhou, China, in 2005 and 2008, respectively, and the Ph.D. degree from the Beijing University of Posts and Telecommunications, Beijing, China, in 2011. He is currently a Professor with Zhengzhou University. His research interests include massive MIMO, cooperative communications, and visible light communication.

KHALED M. RABIE received the B.Sc. degree (Hons.) in electrical and electronic engineering from the University of Tripoli, Tripoli, Libya, in 2008, and the M.Sc. and Ph.D. degrees in communication engineering from The University of Manchester, Manchester, U.K., in 2010 and 2015, respectively. He is currently a Postdoctoral Research Associate with Manchester Metropolitan University (MMU), Manchester. His research interests include signal processing and the analysis of power line, and wireless communication networks. He is also a Fellow of the U.K. Higher Education Academy. He was a recipient of the Best Student Paper Award at the IEEE ISPLC, TX, USA, 2015, and the MMU Outstanding Knowledge Exchange Project Award, in 2016. He is also the Program Chair of the IEEE ISPLC 2018, the IEEE CSNDSP 2018 Co-Chair of the Green Communications and Networks Track, and the Publicity Chair of the INISCOM 2018. He is also an Associate Editor of IEEE ACCESS and an Editor of *Physical Communication* journal (Elsevier).

RUPAK KHAREL (M'09–SM'18) received the Ph.D. degree in secure communication systems from Northumbria University, U.K., in 2011. He is currently a Senior Lecturer with the School of Engineering, Manchester Metropolitan University. His research interests include various use cases and the challenges of the IoT and cyber physical systems (CPS), cyber security challenges on CPS, the energy optimization of the IoT networks for green computing, the Internet of Connected Vehicles (IoV), and smart infrastructure systems. He is also a member of the IET and a Fellow of the Higher Education Academy (FHEA), U.K. He is also a Principal Investigator of multiple government- and industry-funded research projects.